

Methodical Approach for Analyzing Process Variables and Optimizing Boundary Conditions in Multi-Axis Robot Programs

Methodischer Ansatz zur Analyse von Prozessvariablen und Optimierung von Randbedingungen in Multi-Achs-Roboterprogrammen

Scientific work for obtaining the academic degree

Master of Science (M.Sc.)

at the TUM School of Engineering and Design of the Technical University of Munich

Supervised by	Prof. Dr.-Ing. Michael Zäh Institute for Machine Tools and Industrial Management (iwb)
Submitted by	Jan Nalivaika Lerchenauerstrasse 10 80809 Munich
Submitted on	March 01, 2024 in Garching

Acknowledgment

I would like to take this opportunity to express my heartfelt appreciation to my two supervisors, Marius Breuer and Ludwig Siebert, for their exceptional guidance and unwavering support throughout the entire duration of my master's thesis. Their expertise, dedication, and willingness to share their knowledge have been instrumental in shaping the direction and quality of this research. Their valuable insights and constructive feedback have significantly contributed to the development of this work. I am truly grateful for their availability, as they were always approachable and ready to assist whenever I encountered challenges or needed clarification. Their prompt response and timely feedback were incredibly valuable in ensuring the smooth progress of this thesis. I am deeply thankful for their remarkable contributions and for being outstanding mentors throughout this journey.

Scope of Work

Title of the Master's Thesis:

Methodical Approach for Analyzing Process Variables and Optimizing Boundary Conditions in Multi-Axis Robot Programs

Titel der Master's Thesis:

Methodischer Ansatz zur Analyse von Prozessvariablen und Optimierung von Randbedingungen in Multi-Achs-Roboterprogrammen

Author: Jan Nalivaika

Issue: 02.10.2023

Supervisor: Ludwig Siebert

Submission: 01.03.2024

Motivation:

Computer-aided manufacturing (CAM) is used to automatically generate tool paths for computer numerically controlled machines. The CAM software considers the models of the raw and finished parts, the constraints of the machine, the tools, and the manufacturing technology. Together with user-configurable parameters, tool paths for 3-axis, 5-axis, or robot-based machine tools are generated. The growing demand for flexibility in machine tools, such as the use of multiple manufacturing technologies in one machine or automated loading and unloading, has led to many machine tools being equipped with additional mechanical axes. Examples include robots mounted on linear axes and rotary-tilt tables. The tool paths created in CAM programs are usually defined by five degrees of freedom. The first three are the translational axes X, Y, and Z. The tilting and inclining of the tool are defined by the A- and B-axes. Occasionally, an additional rotation of the tool (C-axis) around the Z-axis (e.g., for dragging a swivel knife) is defined. Machines with more degrees of freedom than those limited by the toolpath often need user-defined constraints. These constraints are necessary to fully specify the movements of the machine axes. An example is the alignment of a part using the rotary-tilt table so that the Z-axis of the tool always points in the direction of gravity. This is helpful in processes like fused deposition modeling (FDM) and wire arc additive manufacturing (WAAM). It is common practice to set the user-defined constraints based on experience. The definition of these constraints does not affect the relative tool path generated by the CAM software. A preliminary literature review indicates that the configuration of

these degrees of freedom has an impact on the energy demand and stability of the process. As such, a methodical approach to optimize these constraints in terms of efficiency, speed, and energy demand of the machine is required. Currently, no literature provides a comprehensive analysis or methodology regarding this global optimization problem.

Objective:

This work aims to attain a methodical approach that analyzes a set of constraints and evaluates the influence of those constraints on a set of defined process variables. It will focus on a 6-axis robot with a rotary-tilt table, whereby the results should also be transferable to other machines. Furthermore, the experiments and validations will be limited to the manufacturing processes of WAAM and milling. First, the influence of the constraints on relevant process variables (energy demand, joint turnover, speed and acceleration peaks, and total joint movements) in a manufacturing process such as WAAM will be assessed. Subsequently, a process evaluation will be elaborated in the CAM software, by means of which the process quality can be determined. Depending on the respective process variables, approximation or machine learning methods will be investigated for the process evaluation. The process quality as a one-dimensional variable will be determined by weighting the process variables. Subsequently, a method for the optimization of the constraints will be elaborated. This task corresponds to an optimization problem in which the process quality will be maximized by selecting suitable constraints.

Procedure and working method:

The following work packages are conducted within this thesis:

- Literature research
- Familiarization with WAAM, milling machines, and CAM software
- Selection of suitable process variables
- Elaboration of the proposed method in a suitable programming language
- Verification and validation of the elaborated method
- Documentation of the work

Agreement:

Through the supervision of B.Sc. Jan Nalivaika intellectual property of the *iwb* is incorporated in this work. Publication of the work or transfer to third parties requires the permission of the chair holder. I agree to the archiving of the work in the library of the *iwb*, which is only accessible to *iwb* staff, as inventory and in the digital student research project database of the *iwb* as a PDF document.

Garching, 02.10.2023

Prof. Dr.-Ing.
Michael F. Zäh

B.Sc.
Jan Nalivaika

Abstract

This thesis discusses a method for analyzing process variables and optimizing boundary conditions in manufacturing systems with redundant degrees of freedom (DoF). Strong focus is placed on industrial robots that traverse a toolpath in 5-DoF. This means that while the toolpath defines the X, Y, and Z coordinates, as well as rotations A and B, rotation C is not defined and can be chosen freely. The first part of the methodology covers the analysis of process variables such as direction changes in the joints and total travel of the joints, as well as the influence of the defined boundary condition that constrains the redundant DoF to a specific value. The second part of the method proposes a procedure to optimize the setting of the redundant DoF in order to optimize the user-selected process variables. This problem is analogous to an optimization problem where the process quality is to be maximized. By implementing a PSO algorithm, it is possible to find the most optimal setting for the redundant DoF, thus maximizing the process quality. This procedure shows fast convergence and that it is not necessary to analyze each possible combination of the redundant DoF in a brute-force manner, to find the most optimal setting.

Zusammenfassung

In dieser Arbeit wird eine Methode zur Analyse von Prozessvariablen und zur Optimierung von Randbedingungen in Fertigungssystemen mit redundanten Freiheitsgraden diskutiert. Der Schwerpunkt liegt dabei auf Industrierobotern, die einen Werkzeugweg in fünf Freiheitsgraden abfahren. Das bedeutet, dass der Werkzeugweg zwar die X-, Y- und Z-Koordinaten sowie die Drehungen A und B definiert, die Drehung C jedoch nicht festgelegt ist und frei gewählt werden kann. Der erste Teil der Methode befasst sich mit der Analyse von Prozessvariablen wie Richtungsänderungen in den Gelenken und dem Gesamtverfahrweg der Gelenke sowie dem Einfluss der definierten Randbedingung, die die redundanten Freiheitsgrade auf einen bestimmten Wert beschränkt. Im zweiten Teil der Methode wird ein Verfahren zur Optimierung der Einstellung der redundanten Freiheitsgrade vorgeschlagen, um die vom Benutzer gewählten Prozessvariablen zu optimieren. Dieses Problem ist analog zu einem globalen Optimierungsproblem, bei dem die Prozessqualität maximiert werden soll. Durch die Implementierung eines PSO-Algorithmus ist es möglich, die optimalste Einstellung für die redundante DoF zu finden und damit die Prozessqualität zu maximieren. Dieses Verfahren zeigt eine schnelle Konvergenz und dass es nicht notwendig ist, jede mögliche Kombination der redundanten Freiheitsgrade in einer Brute-Force-Methode zu analysieren, um die optimalste Einstellung zu finden.

Contents

List of Abbreviations	xi
1 Implementation and Validation	1
1.1 Simple Implementation	1
1.1.1 Modeling a 6-DoF Robot	1
1.1.2 Modeling a Basic Toolpath	3
1.2 Testing and Validation	6
1.2.1 Toolpath Evaluation With one Redundant DoF	6
1.2.2 Extracting Process Variables	8
1.2.3 Validation on a Production Grade Toolpath	12
1.2.4 Toolpath Evaluation With two Redundant DoF	15
1.2.5 Boundary Condition Optimization	20
1.3 Analysis and Discussion of the Results	27
1.3.1 Analysis of the Results	27
1.3.2 Discussion of the Results	28
Bibliography	33

List of Abbreviations

CAM	Computer-aided manufacturing
DH	Denavit-Hartenberg
DoF	Degree of freedom
FDM	Fused deposition modeling
PSO	Particle swarm optimization
TCP	Tool center point
WAAM	Wire arc additive manufacturing

Chapter 1

Implementation and Validation

The first step in the validation process involves selecting a manufacturing machine and constructing a fundamental model in the programming language *Python*. In this case, a simple articulated robot is chosen as the manufacturing machine. The programmed model captures the kinematics and dynamics of the modeled industrial robot. It allows for a in depth analysis of its movement and behavior as well as the optimization of its performance.

To test the method in a straightforward scenario, initial tests are conducted on a 6-DoF model with a 5-DoF toolpath. The sixth DoF, which represents rotation around the Z-axis, is freely defined and utilized for optimization purposes. The validation consists of traversing a predefined toolpath and analyzing the individual joint positions over time. Once this simple model is successfully validated, an additional redundant DoF is introduced by incorporating the tilt of a rotary-tilt table.

After establishing the basic model, an optimization algorithm is implemented to determine the optimal values for each redundant DoF in order to optimize the user-selected process variables. This optimization algorithm takes into consideration the specific constraints and objectives of the industrial robot, such as minimizing direction changes or joint accelerations.

The modeled robot, the optimization algorithm as well as the visualizations and plots are constructed using *Python 3.11* with the help of the libraries *visual_kinematics*, *matplotlib* and *numpy*.

1.1 Simple Implementation

1.1.1 Modeling a 6-DoF Robot

To test the proposed method, a simplified articulated industrial robot with 6-DoF is used as a model. A visual representation of this robot modeled in *Python* can be seen in Figure 1.2. The Denavit-Hartenberg (DH) parameters for this robot are provided in Table 1.1. These parameters are essential for describing the geometry and kinematics of the robotic arm. They

define the relationship between adjacent links in the kinematic chain of the robot. The parameter "a" represents the link lengths between adjacent joints. The rotations around the Z-axis between adjacent joints is represented by the parameter "alpha". The parameter "d" represents the link offsets along the Z-axis between adjacent joints. The units of "a" and "d" are in millimeters, while the rotation "alpha" is defined in degrees.

Table 1.1: DH-parameters for the modeled robot

Parameters	Values
a in [mm]	[200, 800, 150, 0, 0, 0]
alpha in [°]	[90, 0, 90, -90, 90, 0]
d in [mm]	[400 0, 0, 600, 0, 200]

The schematic of the modeled robot can be seen in Figure 1.1. In this particular configuration, all joints are in their initial positions with no rotation applied.

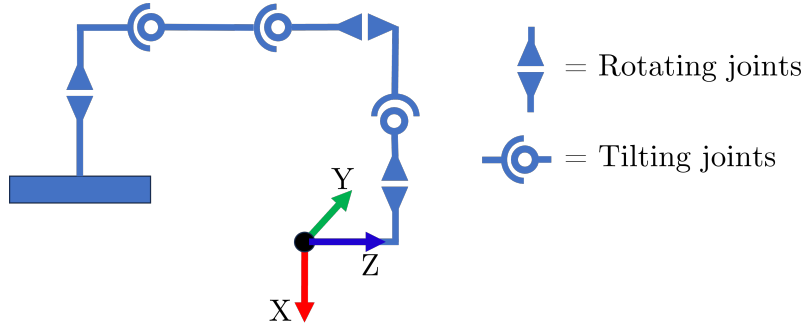


Figure 1.1: Schematics of the modeled robot

Figure 1.2 depicts the modeled robot using *Python* in combination with the *matplotlib* library. The joint positions, in degrees, are as follows: [0, 135, -45, 0, 0, 0], corresponding to joints 1 to 6, respectively. The black coordinate system represents the world coordinate system, while the colored coordinate system originating from the TCP and represents the TCP coordinate system. The first link of the robot, originating from the point X=0, Y=0, Z=0 in the world coordinate system, is displayed in green. The individual joints are represented by red dots. The end-mill is marked as a orange dot.

The next step is to model a spindle that is attached to the flange, which is at the end of the last link, and apply a transformation matrix from the flange to the tip of the end-mill. The length of the spindle is set to 300 mm, and the length of the end-mill is set to 80 mm. The transformation matrix applies a rotation and shift from the coordinate system at the flange, which is determined by the rotation "alpha" (see Figure 1.1), to the tip of the end-mill. This establishes a tool coordinate system at the correct position with the desired orientation.

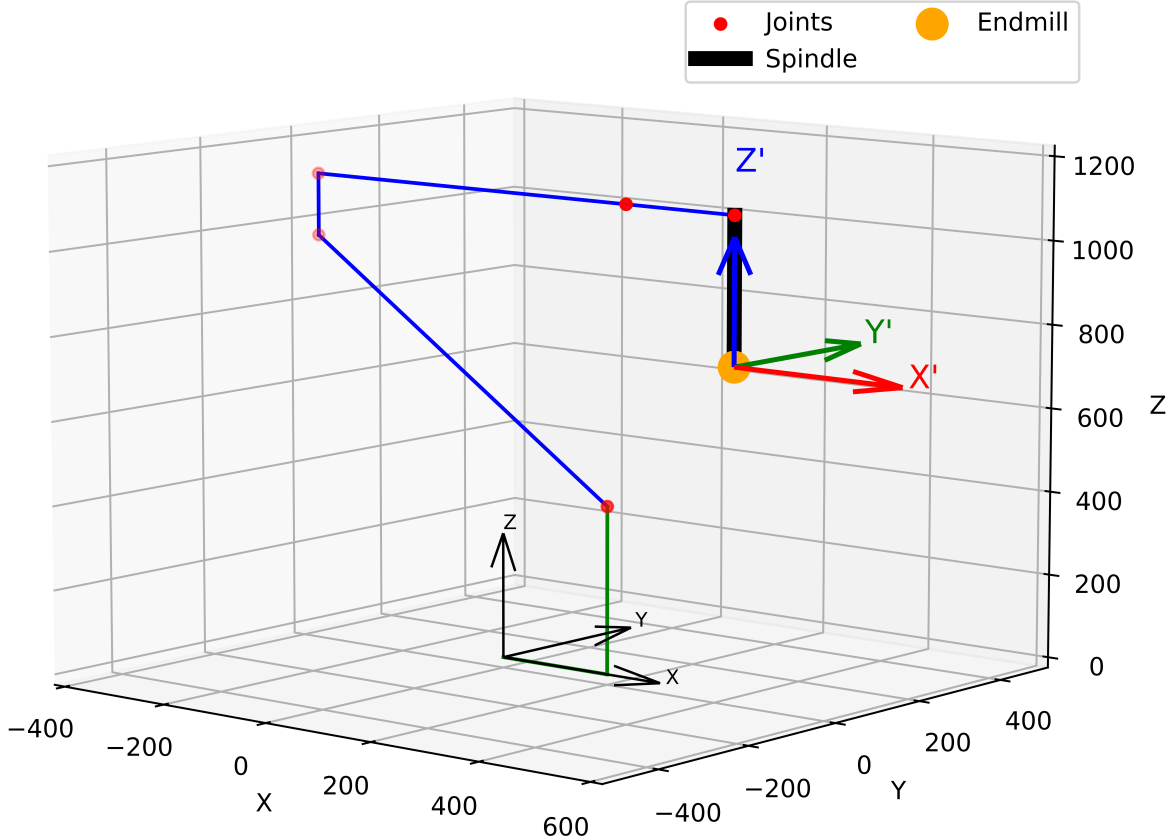


Figure 1.2: Visualization of the modeled robot in Python

1.1.2 Modeling a Basic Toolpath

Before analyzing the process variables of interest, it is necessary to define a toolpath for the TCP to follow. For that case, three exemplary toolpaths are presented, each consisting of 3000 points. To validate the proposed method more broadly, each of those manually created toolpaths has individual characteristics. It should be noted that in the first analysis, the redundant DoF is the rotation around the Z-axis. This rotation will be adjusted to determine the optimal value for the desired outcome. A and B are held at 0°.

The first toolpath, depicted in Figure 1.3, represents a converging spiral that is shifting to the side. Figure 1.4 illustrates the second path which is a converging-diverging infinity-loop, and Figure 1.5 displays a forward-moving sinusoidal curve that is following a parabolic profile. Each path consists out of 3000 coordinates.

Figure 1.6 illustrates the robot and Toolpath 1 at the final position of the toolpath. The origin of the toolpath is shifted by $X=+800$ and $Z=+400$ relative to the world coordinate system. No rotations are applied around the X-, Y-, and Z-axes, resulting in A, B, and C being zero. As a result, the coordinate axes of the TCP are parallel to the axes of the world coordinate system.

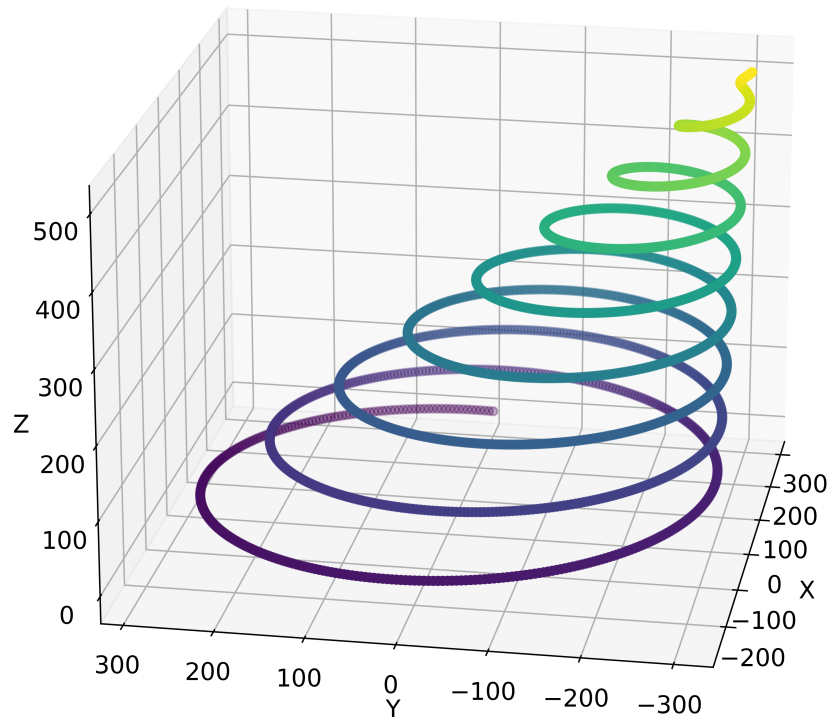


Figure 1.3: Toolpath 1: Converging spiral

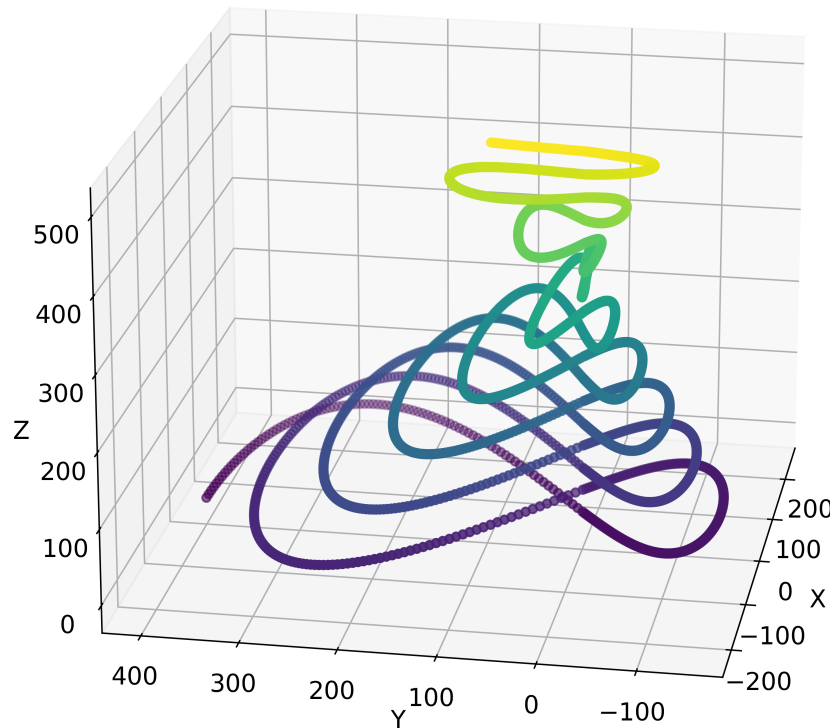


Figure 1.4: Toolpath 2: Converging infinity loop

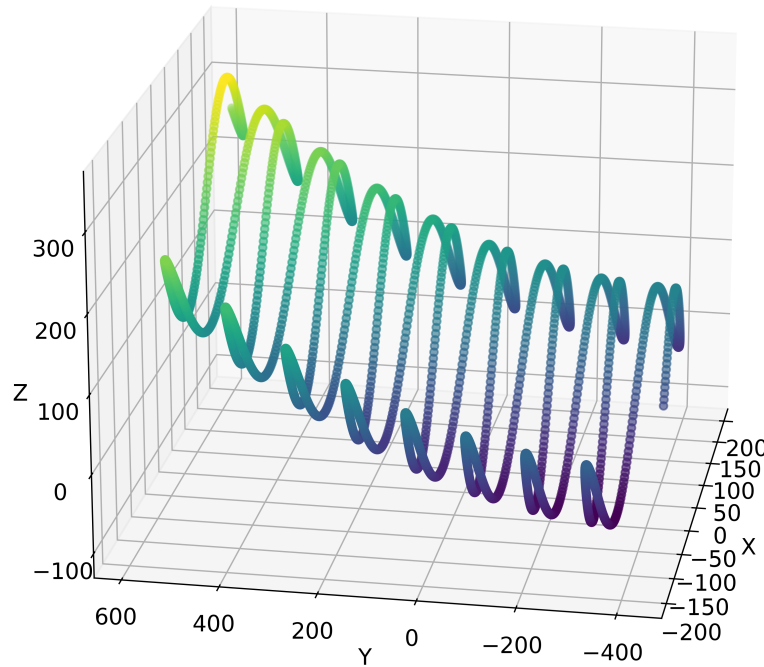


Figure 1.5: Toolpath 3: Forward moving pendulum oscillation

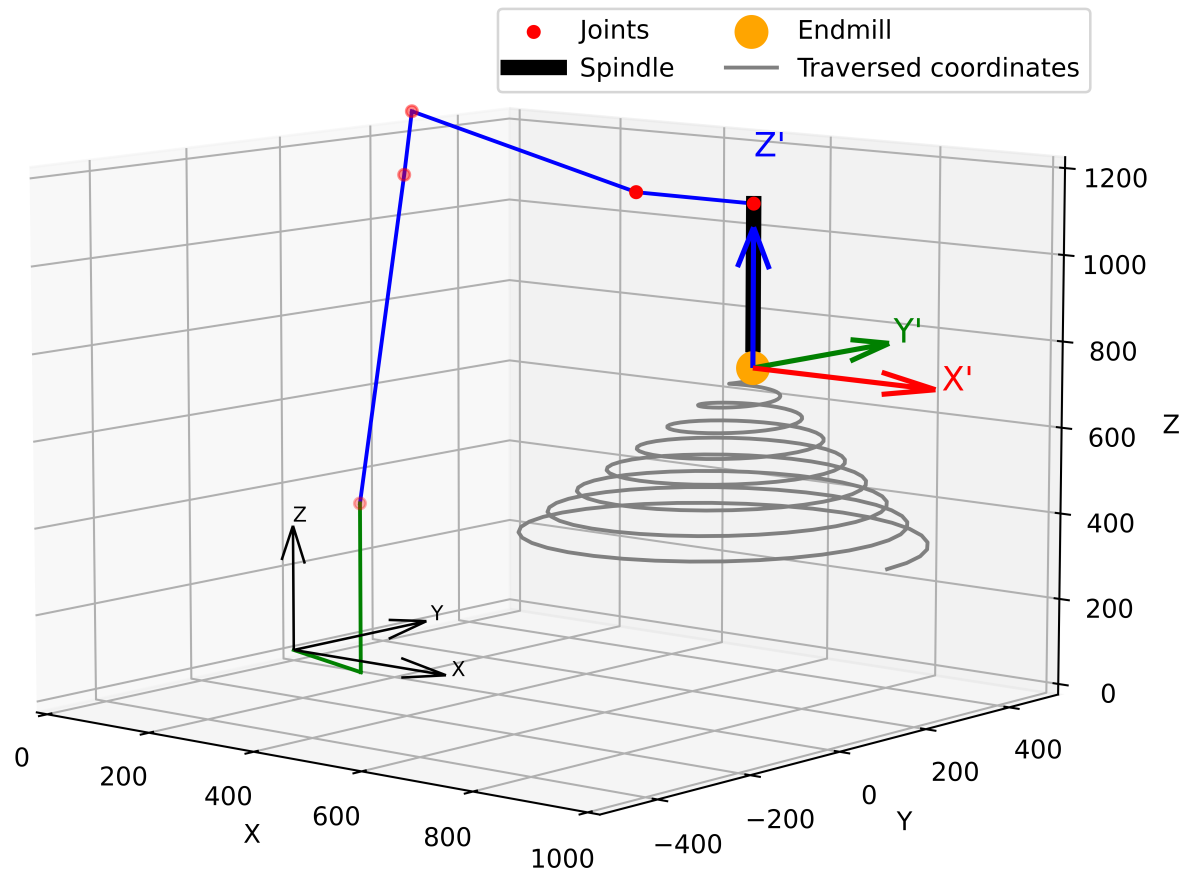


Figure 1.6: Traversing toolpath 1 with the modeled robot

By utilizing the inverse kinematics algorithm from the Python library *visual_kinematics*, the

joint angles for each coordinate can be computed. To achieve this, the rotations A, B, and C need to be defined. The outcome is a time-series that contains the corresponding joint positions. For all tests, all coordinates must be traversed in equidistant time steps. With this information, it becomes possible to calculate the velocity and other related variables. By transforming all the data from the time-series into scalar values and calculating the local rating, the local and global scores can be determined.

1.2 Testing and Validation

1.2.1 Toolpath Evaluation With one Redundant DoF

As discussed in Chapter 1.1.2, the toolpath remains constant with respect to the X-, Y-, and Z-coordinates. The fixed boundary conditions for the robot are that there are no rotations around the X and Y axes, resulting in A and B both being equal to zero. This condition is fixed for the entire toolpath. The user has the ability to set the DoF for the rotation around the Z-axis, which is the redundant DoF. Figure 1.7 displays the variation of each joint over time for toolpath 1. In this specific case, the rotations A, B, and C are all set to 0. The entire toolpath is traversed in 300 seconds.

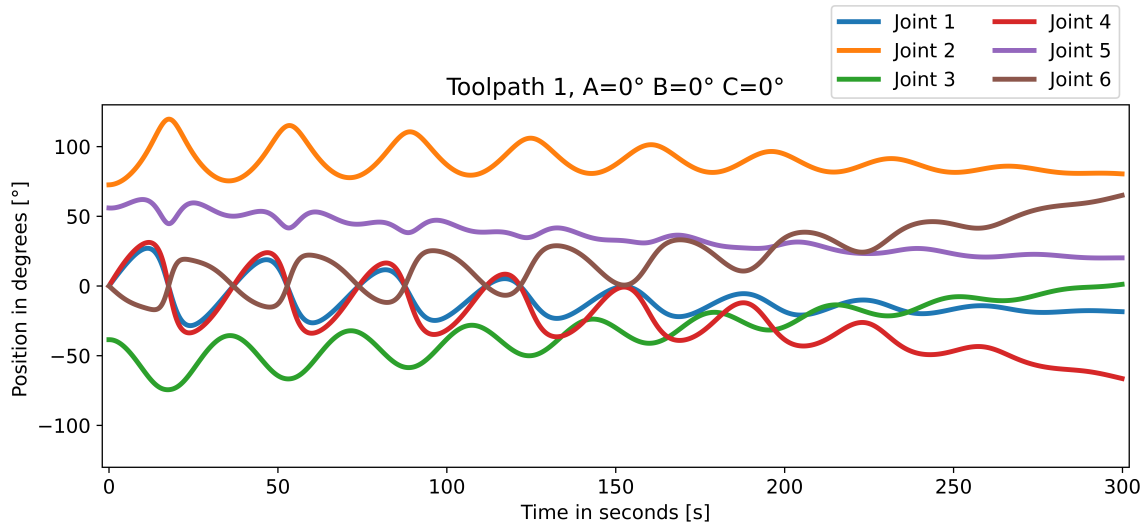


Figure 1.7: Visualization of the joint positions over time for toolpath 1 with $C=0^\circ$

Figure 1.8 depicts the joint positions for all six joints over time for the same toolpath (toolpath 1) with a 45° rotation around the Z-axis ($C = 45^\circ$). It is noticeable that joint 5 and joint 6 have undergone changes in their respective ranges and characteristics. Joint 1 and joint 3 have very similar trajectories in both cases. Additionally, joint 6 exhibits significantly smaller amplitudes at the beginning of the toolpath compared to the case with no rotation ($C = 0^\circ$).

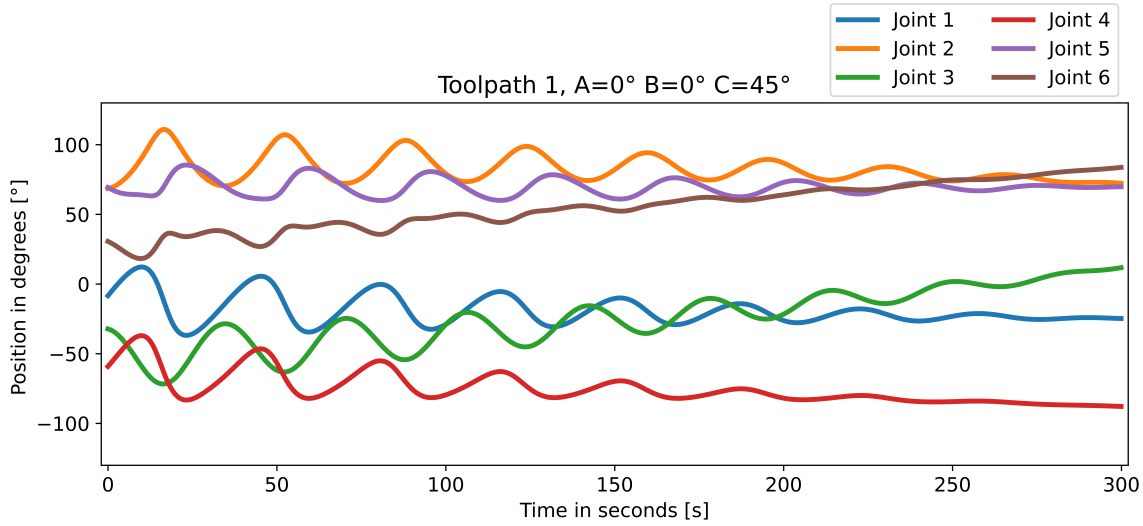


Figure 1.8: Visualization of the joint positions over time for toolpath 1 with C=45°

Figure 1.9 illustrates the variations in each joint over time for toolpath 2 without any rotation (A=B=C=0°). Unlike toolpath 1, the amplitudes in joint 4 and joint 1 noticeably decrease and then increase. This observation aligns with the distinct characteristics of different toolpaths.

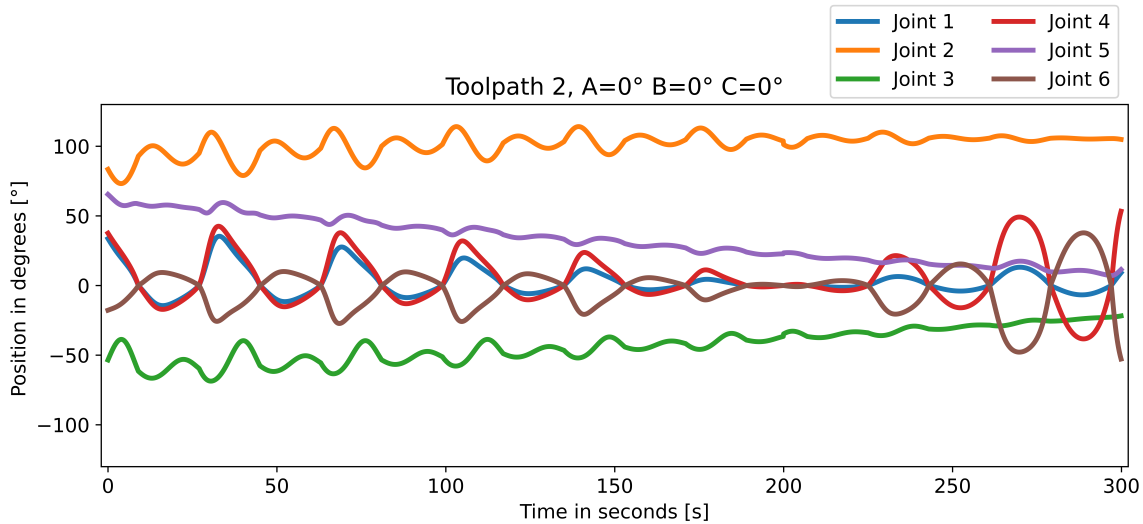


Figure 1.9: Visualization of the joint positions over time for toolpath 2

Figure 1.10 visualizes the variations in each joint over time for toolpath 3. Again, the TCP coordinate system is held parallel to the world coordinate system resulting in A, B and C being zero. A clear oscillation over time is visible in every joint.

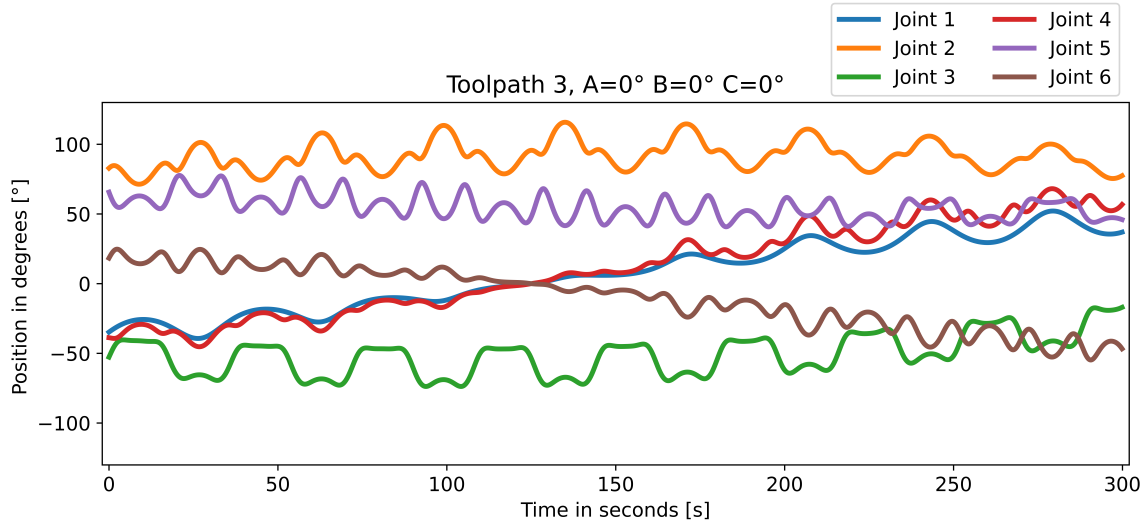


Figure 1.10: Visualization of the joint positions over time for toolpath 3

1.2.2 Extracting Process Variables

The next step involves selecting the process variables of interest and assigning weights to each variable. For this first analysis, a basic case is discussed. As the user has the option to freely choose the process variables, the now chosen ones only serve an exemplary purpose and can be exchanged freely. The same applies to the selected importance factors. Additional process variables can also be added or removed from the analysis.

The selected process variables and importance factors are listed in Table 1.2. The total number of direction changes in all joints and the total distance traveled are chosen due to their ease of implementation. The number of direction changes is assigned an importance factor of 0.2. The total travel in all joints is combined and given an importance factor of 0.4. Additionally, the acceleration of joint 1 is analyzed. To obtain a scalar value for the acceleration, the individual acceleration values are squared and then summed up. The importance factor for acceleration in joint 1 is 0.4. Other process variables are disregarded.

Table 1.2: Selected process variables and their importance factors

Process variables	Importance factors
Direction changes in joints 1-6	0.2
Total travel in joints 1-6	0.4
Acceleration in joint 1	0.4

Since only one redundant DoF is being analyzed, it is possible to represent the individual local scores and global score as a one-dimensional graph. Firstly, toolpath 1 is analyzed by incrementing the redundant DoF (C-axis) by 5 degrees, starting from -135 degrees and ending at 135 degrees.

Figure 1.11 illustrates a case with a -45° rotation around the Z-axis for toolpath 1. Similarly, Figure 1.12 displays a case with a $+45^\circ$. The traversed path is identical but the final pose of the robot and its movements while traversing the path are different.

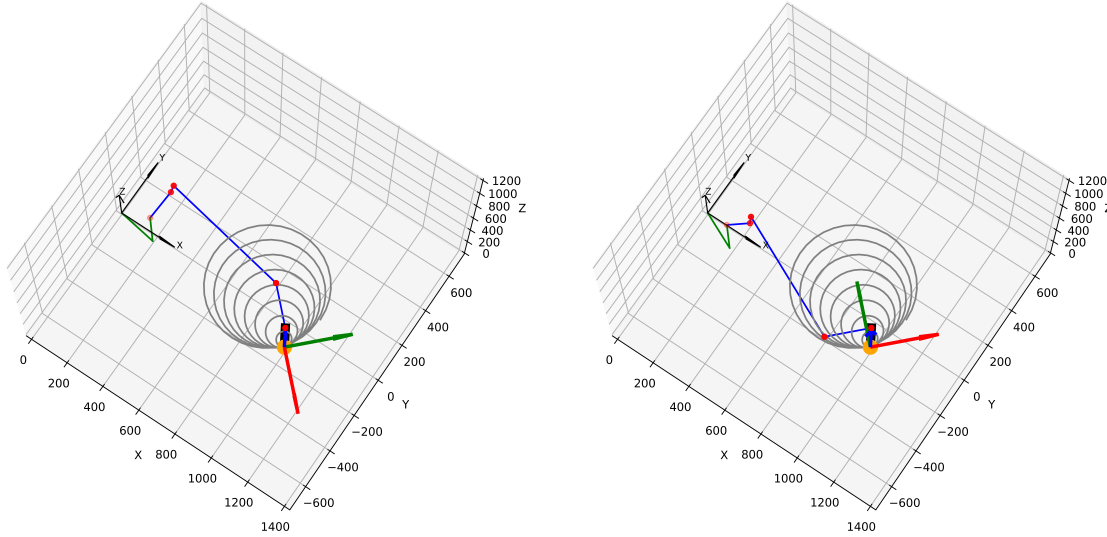


Figure 1.11: Toolpath 1 with $A=0^\circ$, $B=0^\circ$ and $C=-45^\circ$

Figure 1.12: Toolpath 1 with $A=0^\circ$, $B=0^\circ$ and $C=45^\circ$

A total of 55 time-series of joint positions are generated. On average, the inverse kinematics algorithm takes 35 seconds to calculate the joint values for all 3000 coordinates. The process variables are extracted and scaled in relation to each other, as described in Chapter ???. It is important to note that before scaling, the selected process variables are pre-multiplied by -1 , as each value should be minimized. The arrays of local ratings are then multiplied by the weights selected in Table 1.2. Subsequently, the local scores of each process variable can be plotted as a one-dimensional graph, as shown in Figure 1.13.

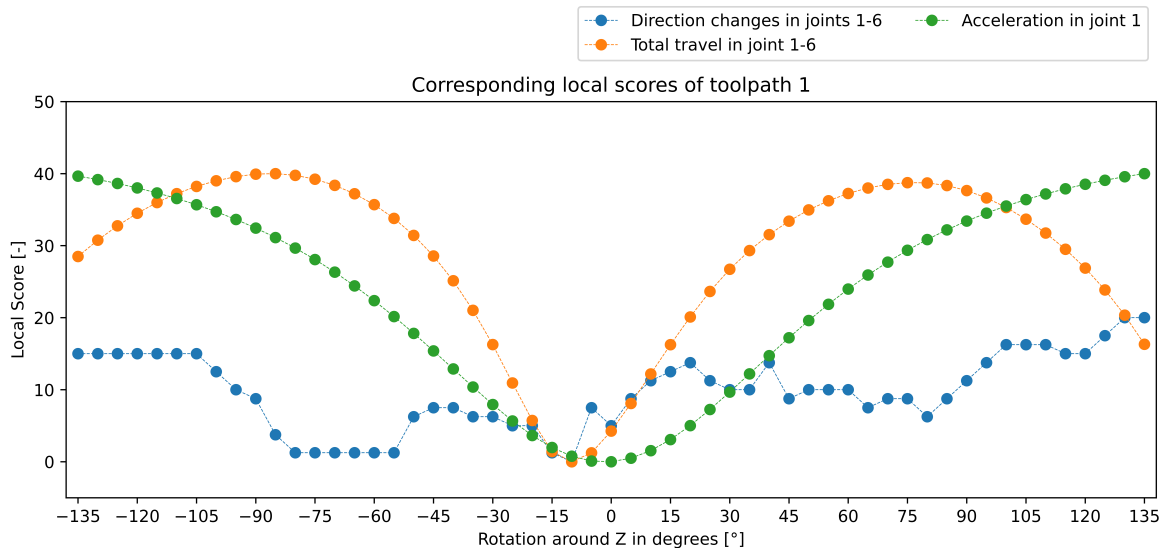


Figure 1.13: Local scores of each process variable for toolpath 1

The acceleration in joint 1 and the combined total travel in the joints display a smooth oscillating curve similar to a sine. The combined travel of the joints is maximized at $C = -10^\circ$, resulting in the lowest local score at that setting. Two maxima (minimal travel) are observed at $C = -80^\circ$ and $C = +75^\circ$. The acceleration in joint 1 exhibits a symmetrical profile, similar to a sine, with the lowest score at $C = 0^\circ$ and two maxima at the two outermost settings. The local score of the direction changes shows a non-smooth progression, with a plateau towards the negative end of the analyzed range. It is worth mentioning that the maximum value that the local score can reach is 40 for acceleration and total travel, while for direction changes, the maximum score is 20. This is due to the assigned importance factors.

Next, the local scores are summed up to calculate the global score. The resulting array, displayed in Figure 1.14, represents the global score achieved by varying the rotation around the Z-axis in relation to all other analyzed values. The orange star on the graph indicates the maximum attainable score and its corresponding rotation, compared to all analyzed boundary conditions.

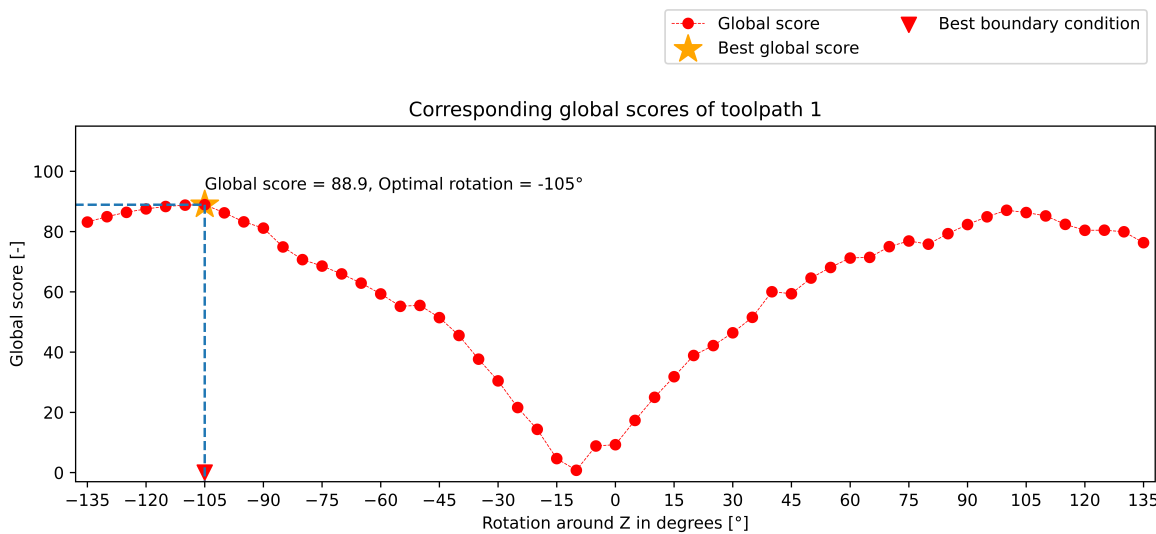


Figure 1.14: Global score for toolpath 1

In this particular case, the highest achievable score is 89.9 at -105° degrees. This score indicates that setting the rotation C to -105° degrees results in close to minimal direction changes, almost minimal total travel, and close to minimal acceleration in joint 1. It is crucial to emphasize that this rating is only in comparison to the other analyzed boundary conditions.

The same analysis, using identical process variables and weights, can be performed with toolpath 2 and toolpath 3. Figure 1.15 and Figure 1.16 display the global and local scores for each analyzed value of the redundant DoF. For toolpath 2, the best score is 89.6 at $C=135^\circ$, while for toolpath 3, the best score is 93.5 at $C=105^\circ$.

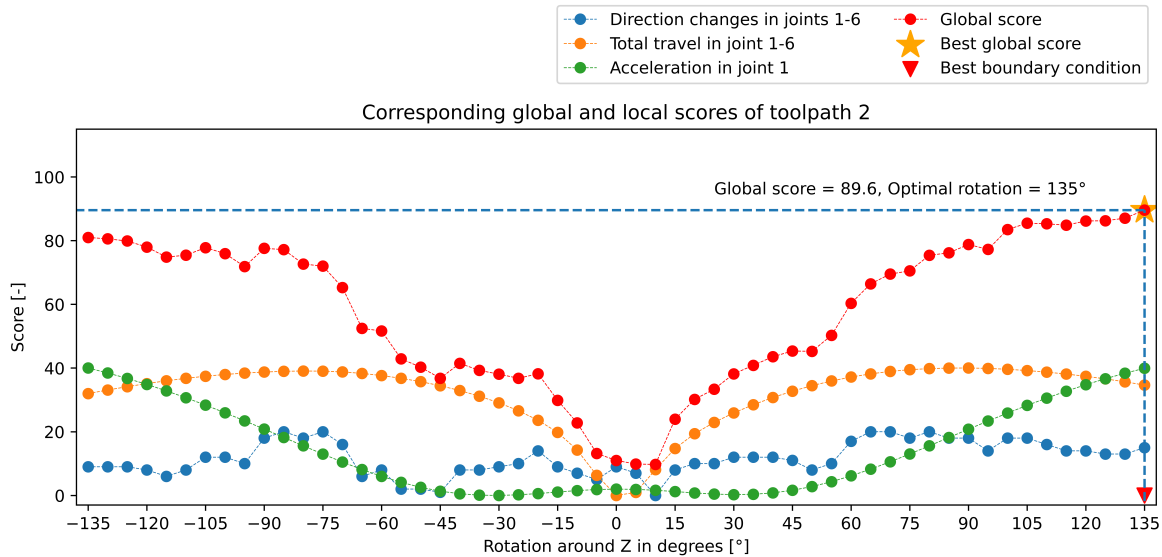


Figure 1.15: Global and local scores in toolpath 2 depending on the rotation around Z

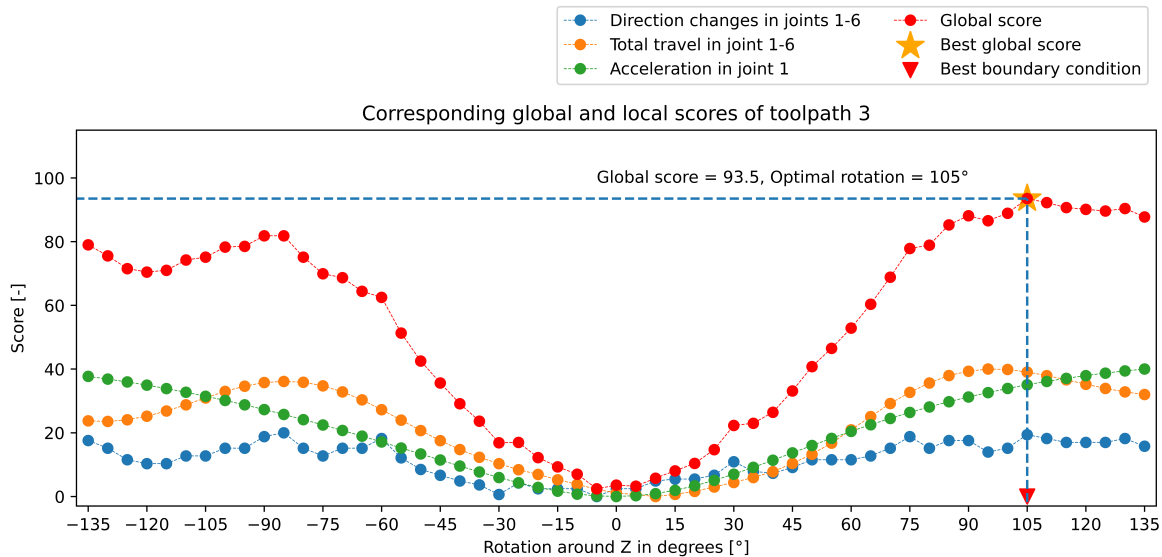


Figure 1.16: Global and local scores in toolpath 3 depending on the rotation around Z

It is noteworthy that even though all toolpaths have significantly different characteristics, all global scores analyzed process variables show a similar trend. The total travel and acceleration show a smooth and almost symmetric characteristic. High global scores are achieved by setting the rotation to high positive or high negative numbers, while low scores are achieved by setting the rotation close to 0°. This might be due to the robot's configuration, where the joints hinder the robot's movements. To continue on the predefined path, the robot has to quickly adjust the joints and reorient them to traverse the toolpath in the same time.

Additionally, it is important to note that when a local score reaches its maximum value, it does not imply that the corresponding variables, such as the number of direction changes, become zero. Instead, it signifies that the number of direction changes is at its lowest compared to

all other analyzed options. Based on the results, it is reasonable to conclude that optimizing the redundant DoFs can significantly improve the manufacturing process.

1.2.3 Validation on a Production Grade Toolpath

In addition to the three simulated toolpaths, a toolpath that was used for the production of a WAAM component is now being used for validation. The toolpath has an organic structure that requires tilting of the rotary-tilt table to ensure that the material deposition process occurs in the direction of gravity. Thus, the position of the rotary-tilt table is not horizontal during the process. The redundant DoF remains the rotation around the Z-axis of the tool, as before. Figure 1.17 provides a visual representation of the analyzed toolpath. It consists of 28,000 coordinates and is modeled to be traversed in 2,800 seconds.

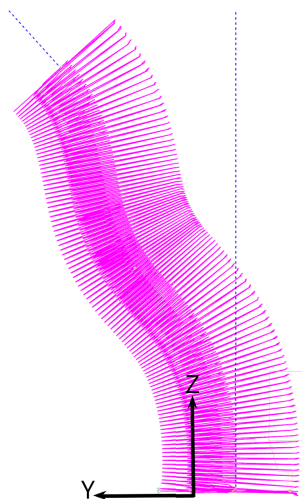


Figure 1.17: Organic toolpath (Reisch 2023)

The process variables for the analysis of this toolpath are defined in Table 1.3. As before, the selected process variables just serve a exemplary purpose and can be exchanged freely by the user. For the following, new process variables are selected compared to the first analysis (see Table 1.2), to further validate the elaborated method.

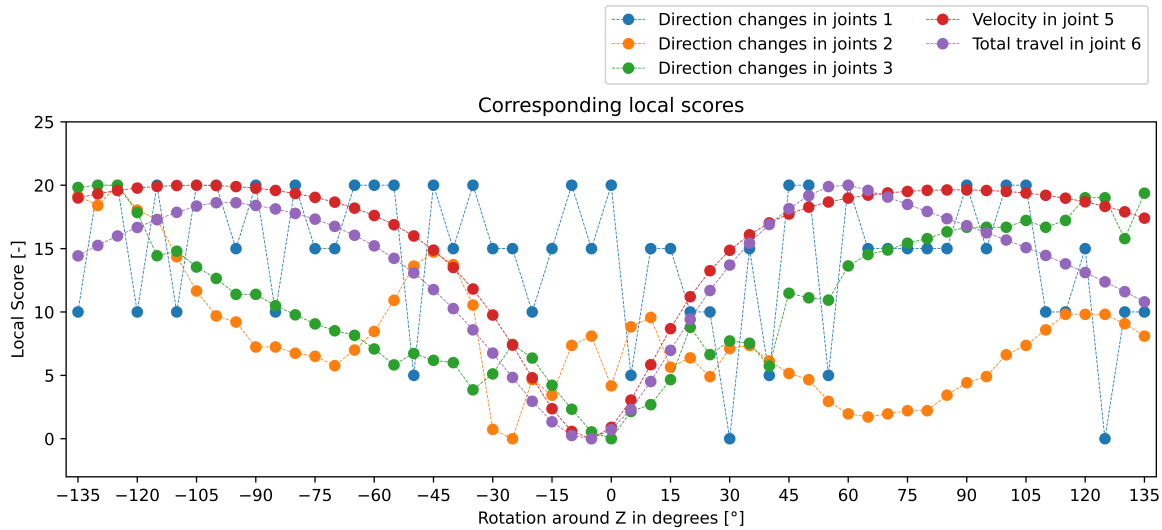
In this example, the direction changes in joints 1, 2, and 3 are all individually weighted with a factor of 0.2. The last two variables are the velocity in joint 5 and the total travel in joint 6. These variables are also weighted with an importance factor of 0.2. To obtain a scalar value for the velocity, all elements of the time-series are squared and summed up.

Table 1.3: Selected process variables and their importance factors for the organic toolpath

Process variables	Importance factors
Direction changes in joint 1	0.2
Direction changes in joint 2	0.2
Direction changes in joint 3	0.2
Velocity in joint 5	0.2
Total travel in joint 6	0.2

The redundant DoF is once again analyzed in 5° increments, starting from -135° and ending at 135° . The resulting local scores are shown in Figure 1.18. It is evident that the velocity in joint 5 and the total travel in joint 6 exhibit a smooth and almost symmetrical behavior. The direction changes in joint 2 and 3 exhibit smooth progression in some section but are significantly jerkier than the analyzed velocity and total travel. When examining the local score of joint 1, it is apparent that the individual scores only fall at 0, 5, 10, 15, or 20. This artifact arises from the fact that the direction changes in joint 1 can only reach five distinct equidistant numbers, which are: 630, 632, 634, 636, and 638. These values differ by a very small percentage relative to each other.

The difference in the count of direction changes can be attributed to the implemented process of calculating the joint angles in the inverse kinematics algorithm. The algorithm terminates the iterative calculation of the joint angles if the TCP is within 0.00001 mm of the defined coordinate. This can introduce rounding errors that result in different outcomes for process variables, even though the same number was expected.

**Figure 1.18:** Global and local score for WAAM toolpath

When analyzing the standard deviation of the individual process variables, as shown in Table 1.4, the stark contrast between them becomes apparent. To calculate the standard deviation of a process variable, all the individual values achieved by setting the redundant DoF to

the discrete analyzed values are utilized. It is important to note that the standard deviation is calculated based on the physical values before applying the Min-Max Scaler, rather than on the local score itself.

As mentioned in Chapter ??, the standard deviation of the direction changes in joint 1 is not sufficient to contribute to the analysis and optimization of the boundary condition. Therefore, this process variable is omitted from further analysis. It is worth noting that the higher the standard deviation of a process variable, the greater the potential for improvement in a physical sense. However, it is important to recognize that the global score is only influenced by the selected importance factors and does not take into account the physical nature of the process variables. The physical nature of the process variables is only reflected in the standard deviation.

Table 1.4: Standard deviation of the selected process parameters

Process variables	Standard deviation
Direction changes in joint 1	2.166
Direction changes in joint 2	38.513
Direction changes in joint 3	62.301
Velocity in joint 5	14795.394
Total travel in joint 6	546.560

Figure 1.19 illustrates the combined local scores in the form of the global score without the addition of the direction changes in joint 1. The highest global score is 75.6, which is achieved by setting the C-axis to -125°. The fairly smooth progression of the global score in all analyzed toolpaths, serves as a strong indicator that an optimization algorithm will easily find an optimum setting for the redundant DoF.

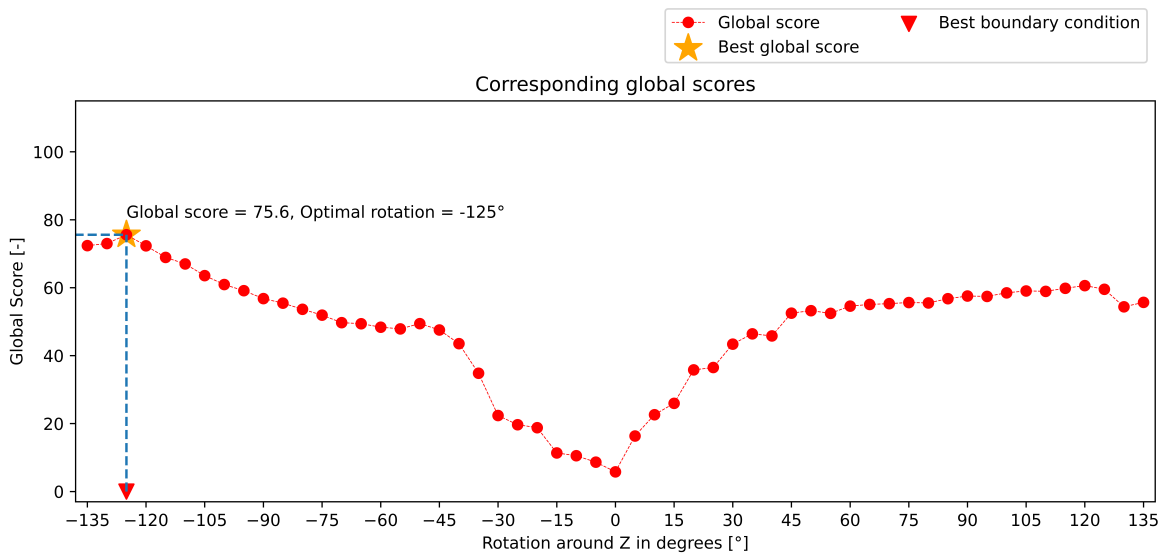


Figure 1.19: Global score for production toolpath

1.2.4 Toolpath Evaluation With two Redundant DoF

To introduce an additional redundant DoF, a rotary-tilt table is simulated. Currently, only the tilting element is being analyzed. All coordinates of the toolpath can be rotated by a specified degree around the X-axis of the toolpath coordinate system. Figure 1.20 depicts toolpath 3 with no rotation around the X-axis, while Figure 1.21 illustrates a rotation of +25 degrees.

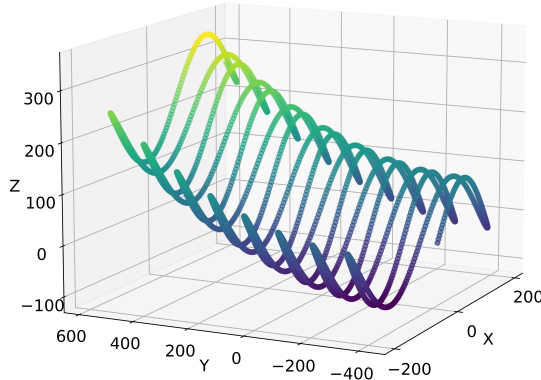


Figure 1.20: Toolpath 3 with no rotation around the X-axis

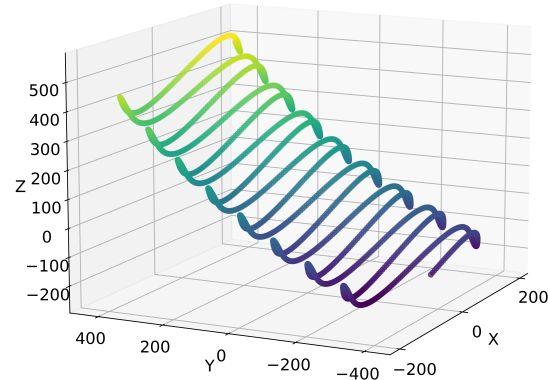


Figure 1.21: Toolpath 3 with a rotation of 25 degrees around the X-axis

Similar to the previous analysis, the same steps need to be followed. The newly selected process variables are presented in Table 1.5. The direction changes of the tilting joints (2+3+5) are combined and treated as one process variable, weighted with a factor of 0.3. Direction changes in joint 1 and acceleration in joint 4 are considered as individual variables, both individually weighted with 0.25. The final variable is the velocity in joint 6, weighted with 0.2. Just as before it is important to reiterate that these process variables serve a exemplary purpose and can be grouped and exchanged as desired.

Table 1.5: Selected process variables and their importance factors for two redundant DoFs

Process variables	Importance factors
Direction changes in joints 2+3+5	0.3
Direction changes in joints 1	0.25
Acceleration in joint 4	0.25
Velocity in joint 6	0.2

Figure 1.22 displays the robot and its orientation while following the tilted toolpath 3. It is crucial to note that since the toolpath is defined in 5 DoFs in its own frame, the frame of the TCP must also tilt by the same degree as the table. The two redundant DoFs in this

case are the rotation around the Z-axis in the frame of the tilted toolpath and the tilting of the toolpath itself. This introduces an additional dimension, as now two parameters can be adapted for optimization.

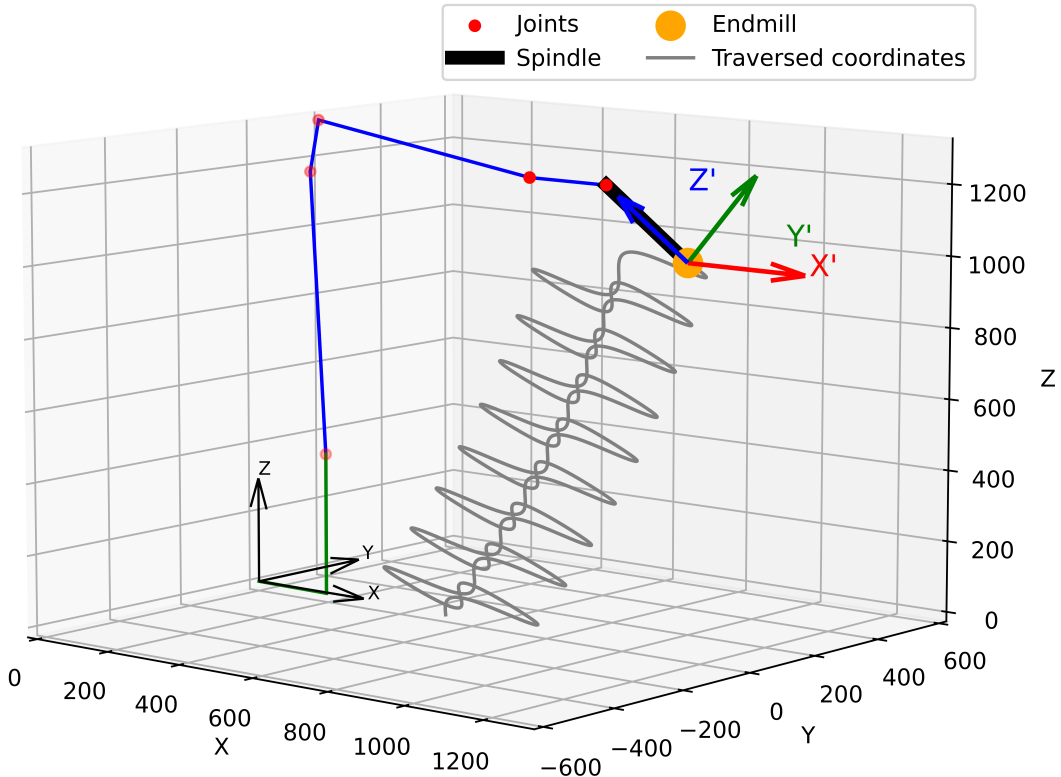


Figure 1.22: Robot following the tilted toolpath 3

The range of possible tilt positions ranges from -45° to 45° in 2-degree increments. For every combination of tilt and rotation, the joint angles are generated using inverse kinematics. To speed up the computation, only every third coordinate is utilized in the inverse kinematic algorithm. This reduces the toolpath by 2000 points and speeds up calculation time. On average, it now takes only 10 seconds to calculate the joint positions. A total of 2530 individual combinations are analyzed.

The extracted process variables are again multiplied by -1, as the objective is to minimize them. Afterwards, the Min-Max scaler is applied. The individual values are aggregated and presented in the form of a matrix. The values of this matrix are visualized in Figure 1.23. The maximum achievable score from all possible combinations is 85.4, visualized by the red cross. This score was attained by setting the table tilt to -1° and the rotation around the Z-axis of the tool to $+115^\circ$. The resulting hyperplane exhibits two distinct local maxima. The entire surface displays a smooth curvature.

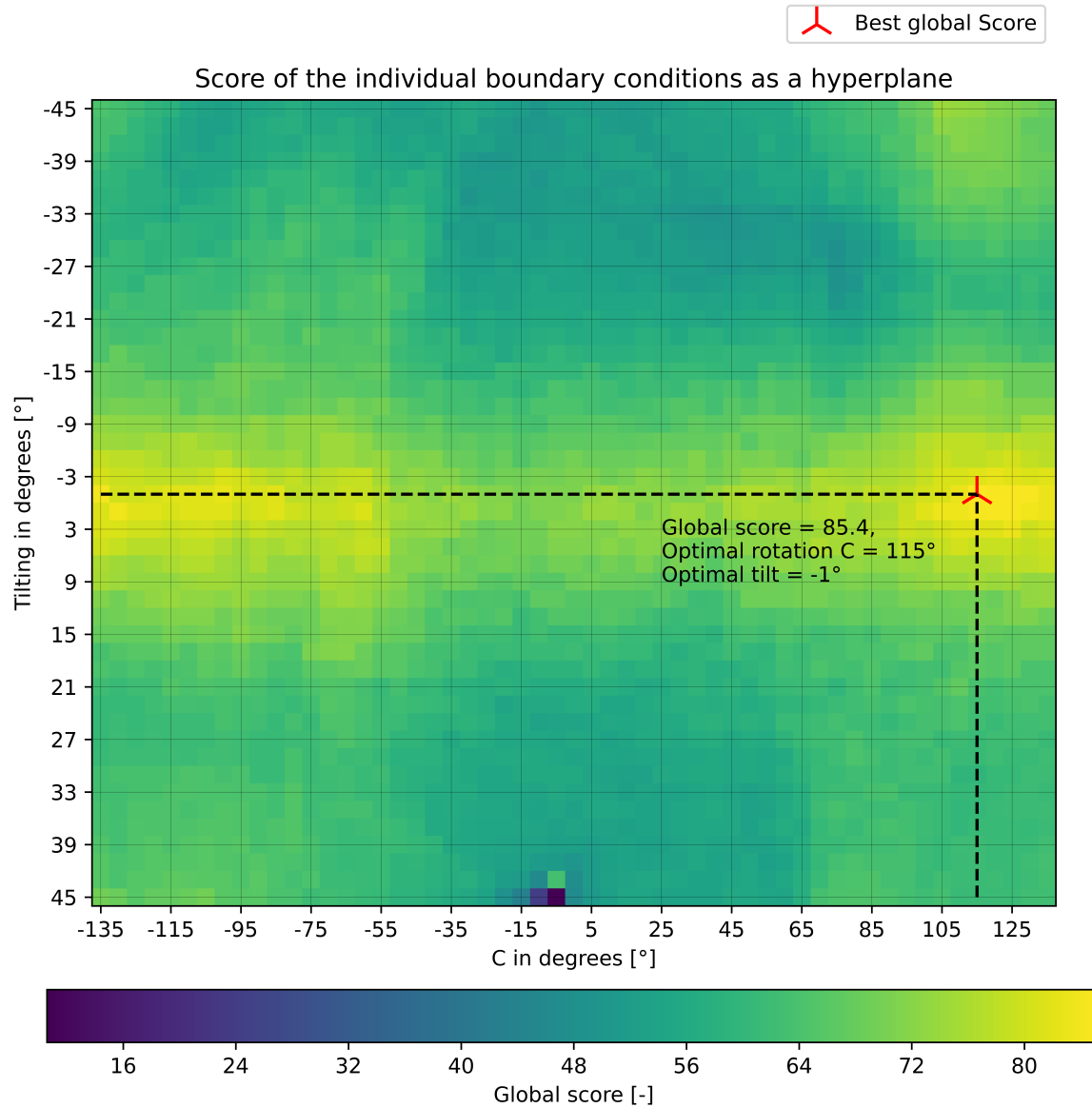


Figure 1.23: Hyperplane representing the global score of toolpath 3

The same analysis is performed with toolpath 1 and toolpath 2. The resulting matrix of the global scores for each possible boundary condition combination is shown in Figure 1.24 and Figure 1.25, respectively. The same process variables and weights (see Table 1.5) are used for the calculations.

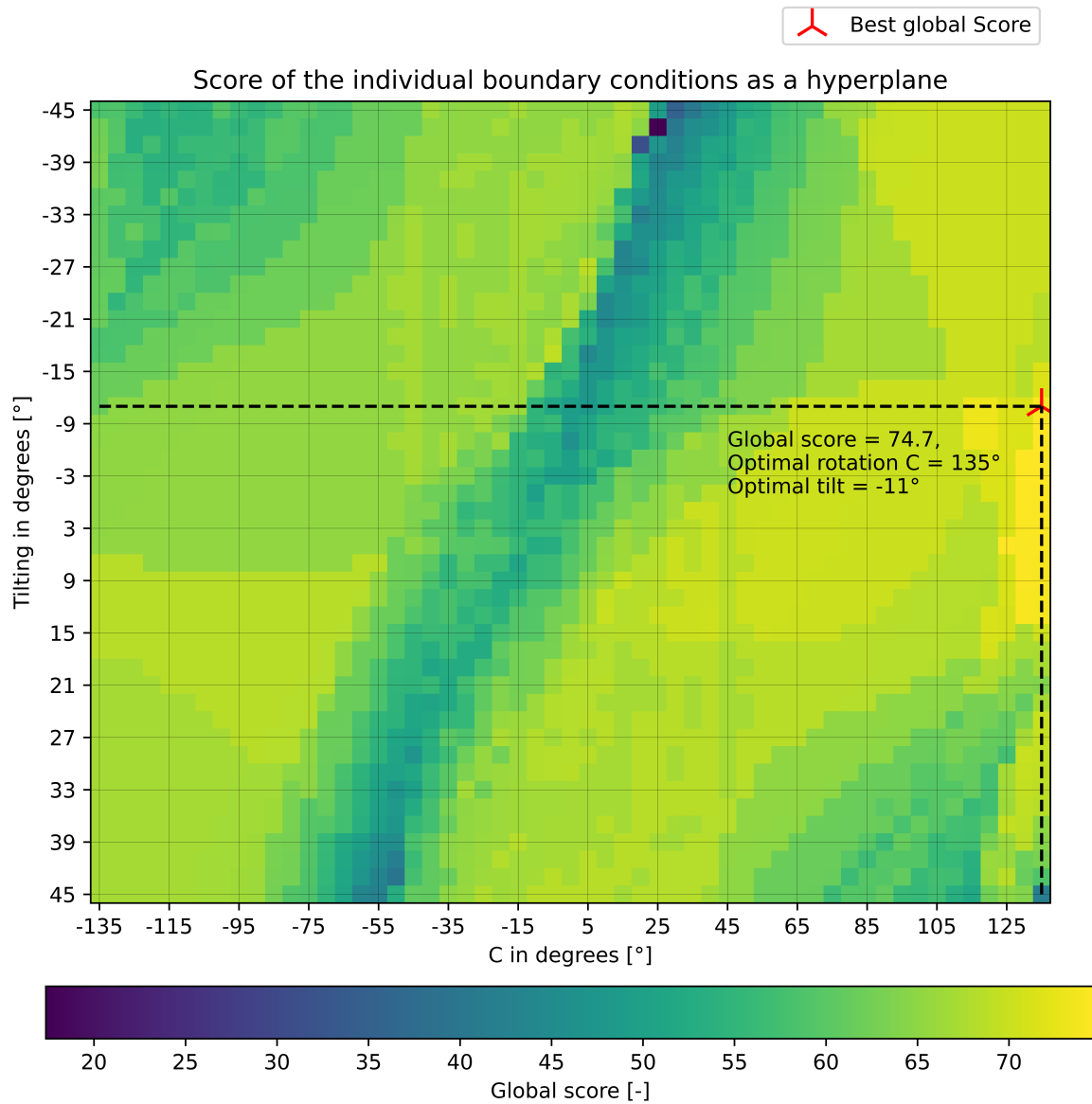


Figure 1.24: Hyperplane representing the global score of toolpath 1

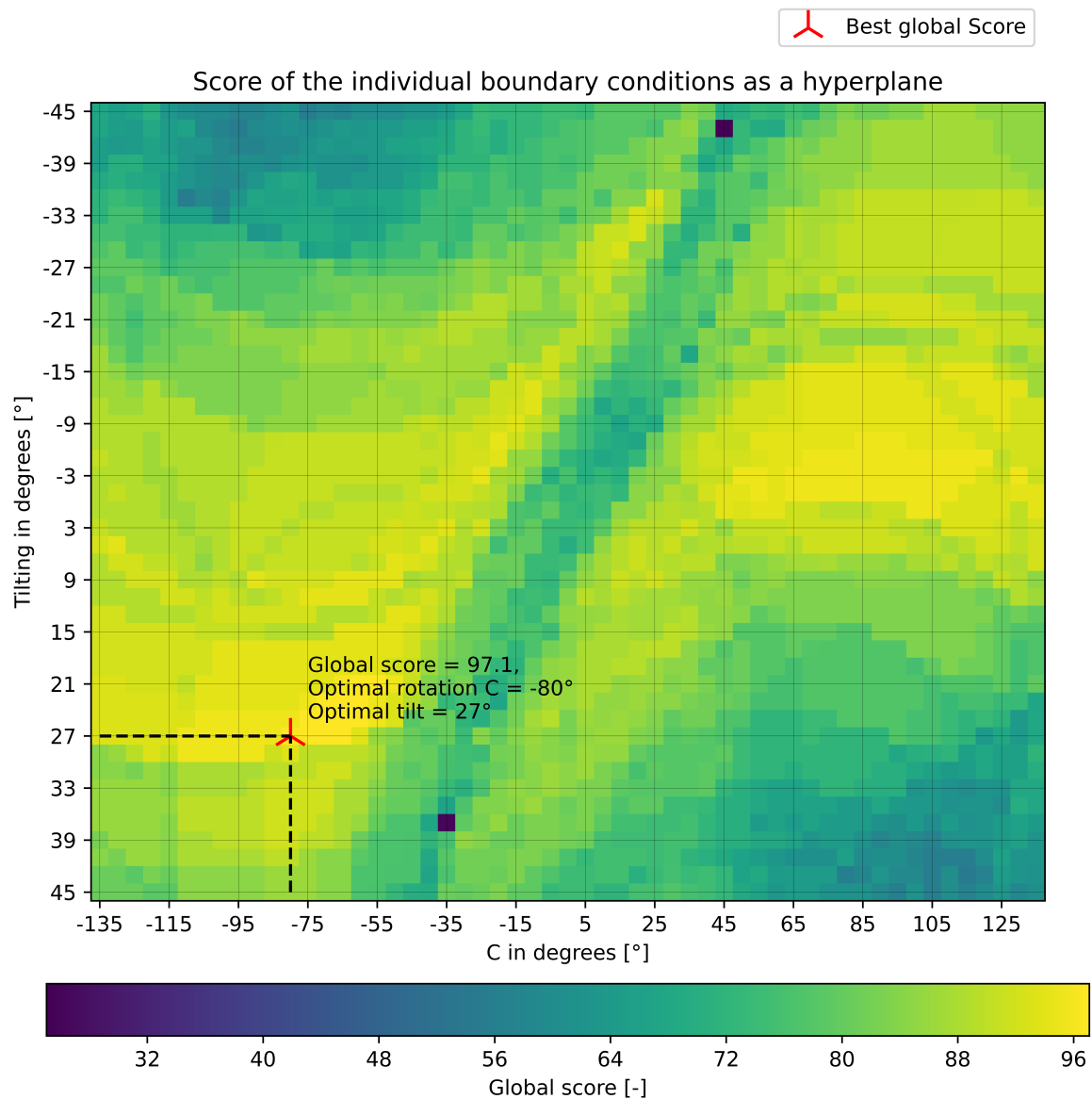


Figure 1.25: Hyperplane representing the global score of toolpath 2

1.2.5 Boundary Condition Optimization

So far, only the analysis of different boundary conditions has been performed by exploring the entire range of possible settings for the redundant DoFs. However, this approach is very time-consuming and becomes exponentially more complex with additional redundant DoF and a finer step size. To address this issue and efficiently search the extensive solution space for optimal values of the redundant DoF, a PSO algorithm is proposed. In this algorithm, individual particles navigate the search space by adjusting their positions based on their own best position and the best position found by the entire swarm.

In more detail, each particle in a swarm optimization algorithm has an initial velocity, which represents its momentum or tendency to continue moving in the same direction. This velocity is adjusted based on several factors, including its current velocity, its own historical best position, and the best-known position of the entire swarm.

The mathematical procedure for adjusting the velocity of a particle is represented by the equation 1.1. In this equation, $velocity_{current}(t+1)$ is the updated velocity of the particle at time $t+1$. $velocity_{current}(t)$ is the current velocity of the particle at time t . $c1$ and $c2$ are cognitive and social constants, respectively, which are both typically set to 1. $r1$ and $r2$ are random values in the range $(0,1)$. $position_{individualbest}$ represents the particle's own historical best position, and $position_{globalbest}$ represents the best-known position of the entire swarm.

Additionally, the equation includes an inertia weight, denoted as w . This weight is used to balance the exploration and exploitation capabilities of the algorithm. A higher inertia weight allows for more exploration, while a lower inertia weight promotes exploitation. In most cases, the inertia weight is set to a value of 0.4.

$$\begin{aligned}
 velocity_{cognitive}(t) &= c1 * r1 * (position_{individualbest} - position_{current}(t)) \\
 velocity_{social}(t) &= c2 * r2 * (position_{globalbest} - position_{current}(t)) \\
 velocity_{current}(t + 1) &= w * velocity_{current}(t) + velocity_{cognitive}(t) + velocity_{social}(t) \\
 position_{current}(t + 1) &= position_{current}(t) + velocity_{current}(t + 1)
 \end{aligned} \tag{1.1}$$

This procedure is iteratively applied to each particle in the swarm. This cooperative behavior enables the particles to explore the search space more effectively and converge towards the best solution (see Chapter ??).

The first test is conducted using the global score matrix of toolpath 3. Initially, 20 particles are randomly placed on the plane. Each particle's score is determined by the corresponding global score at its position. By increasing the number of particles and iterations, the search space can be analyzed more comprehensively. Figure 1.26 illustrates the randomly placed particles on the pre-calculated global score matrix of toolpath 3, considering the previously selected importance factors (see table 1.5).

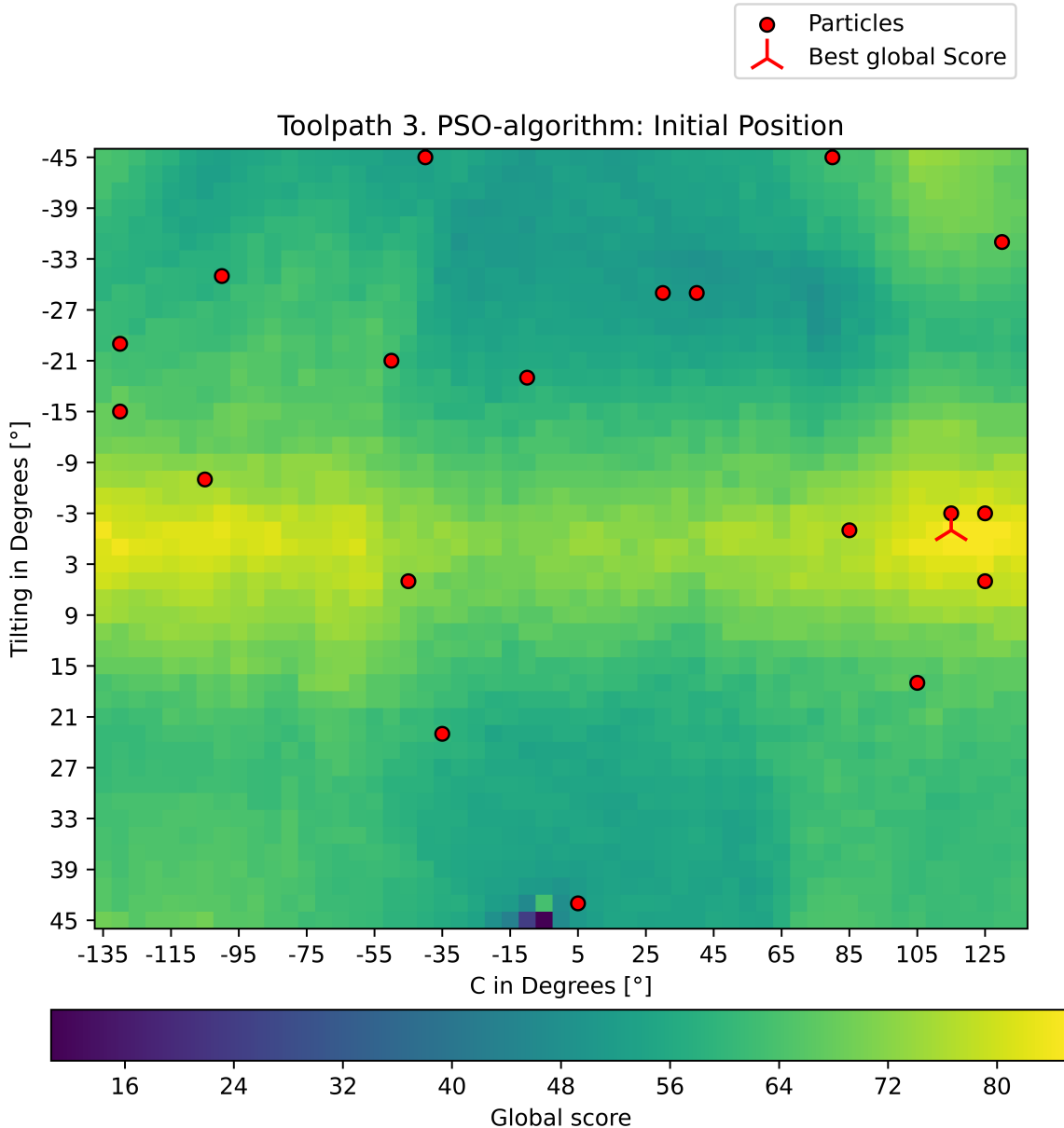


Figure 1.26: Distributed of particles at their initial positions

It is important to clarify that the individual particles in the PSO algorithm do not have access to the entire global score matrix. The visualization of the global score matrix is only provided for the benefit of the human reader to aid in understanding. In reality, each particle only has knowledge of the global score at its own position. The particles update their positions iteratively by comparing their positions with each other. Each particle determines a new position based on the best score observed so far by all particles and the best score observed by itself.

Figures 1.27 to 1.30 demonstrate the convergence of the particles towards the maximum global score. This convergence is achieved within 5 iterations. It is noteworthy that the best position of all 20 particles corresponds to the global maximum, as discussed in Chapter 1.2.4.

This example highlights the ability to explore a high-dimensional space without the need to compute all possible combinations.

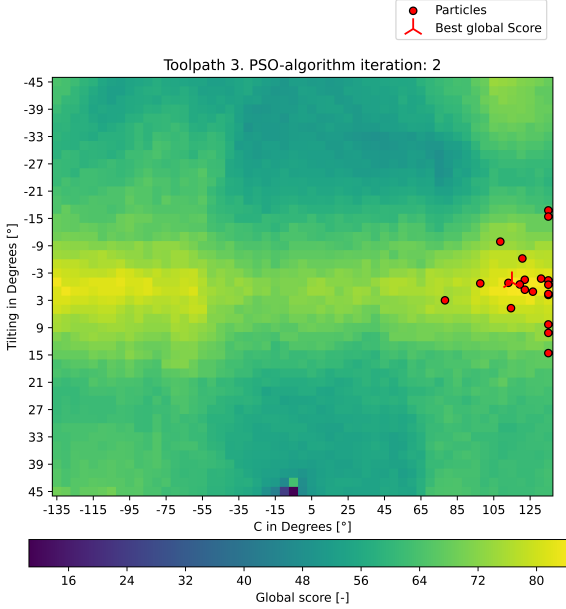


Figure 1.27: PSO Iteration 2 on toolpath 3

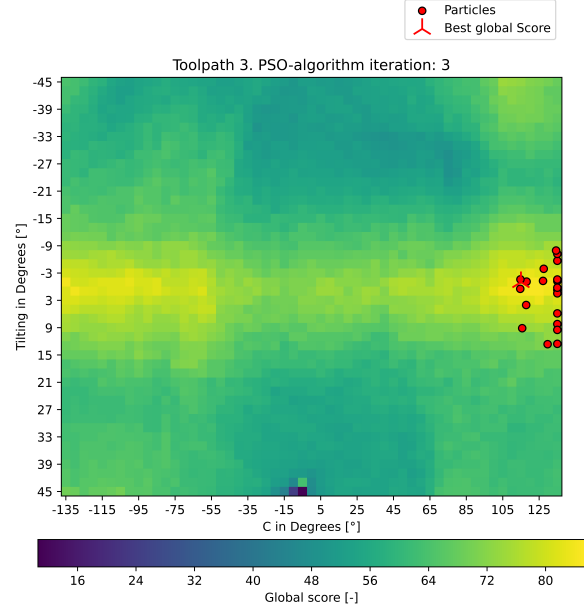


Figure 1.28: PSO Iteration 3 on toolpath 3

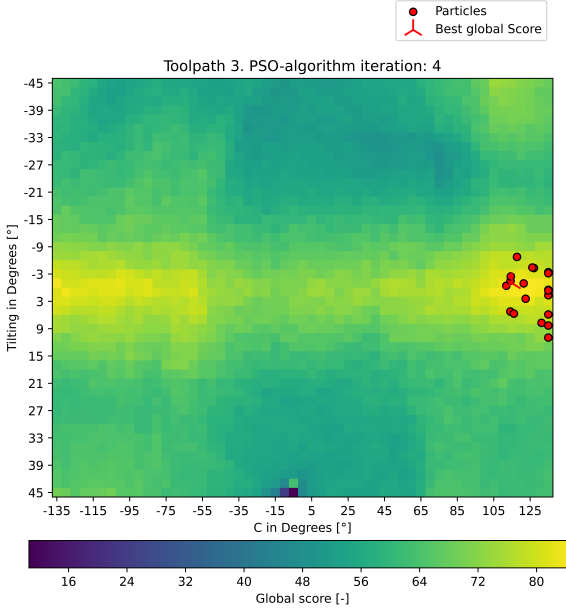


Figure 1.29: PSO Iteration 4 on toolpath 3

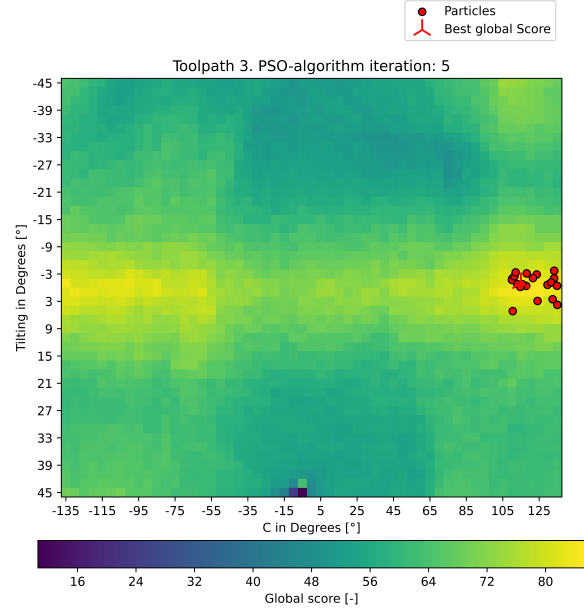


Figure 1.30: PSO Iteration 5 on toolpath 3

One important consideration in this test is, that the scores have already been calculated. The global score matrix is determined by evaluating all possible combinations of different boundary conditions. However, in the intended scenario where this method is used to find the optimal boundary condition, such a pre-calculated matrix does not exist.

Therefore, in each iteration, the scores of the individual particle positions need to be com-

pared relative to each other, taking into account the previous iterations. This process is illustrated in Figure 1.31. Initially, a predetermined number of particles is randomly placed on the plane, with the X and Y values representing the selected boundary conditions. For each selected boundary condition, the joint angles are calculated using the inverse kinematic approach. The analyzed process variables are then extracted and the joint angles are stored. The score for each current position is calculated relative to all other stored toolpaths.

It is possible that in an early iteration, a particle had a position with a significantly higher score compared to the other available toolpaths. Therefore, after each iteration, it is necessary to update the score of the particle's most optimal position as more boundary conditions are analyzed. This is done to ensure that a score, which may have been mistakenly chosen as the best, does not influence the subsequent search directions.

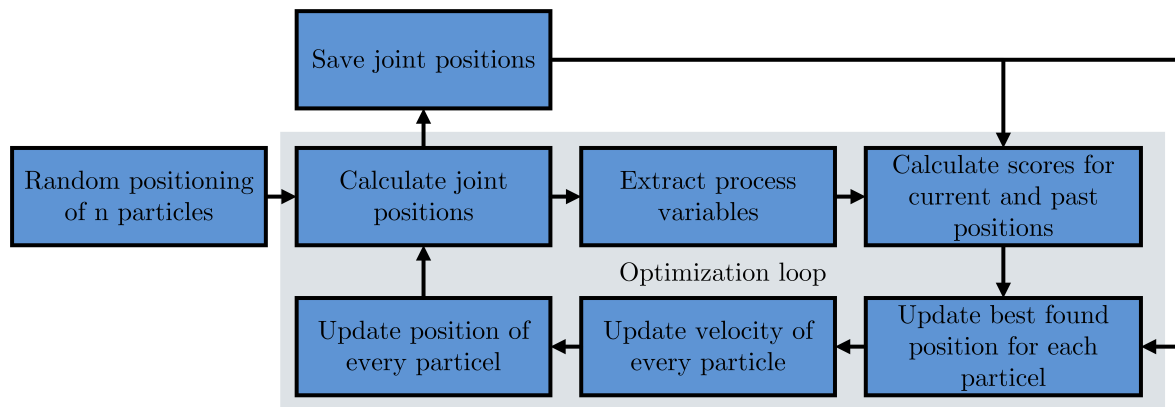


Figure 1.31: PSO-Loop

By utilizing this approach, the following results have been obtained. It is important to emphasize that the precalculated values of the global score matrix are not accessible to the PSO algorithm. They are only used for evaluating the behavior of the particles and aiding in visualization. Figures 1.32 to 1.35 illustrate the evolution of the individual particles. The green circle represents the overall best position discovered by the particles up to that point.

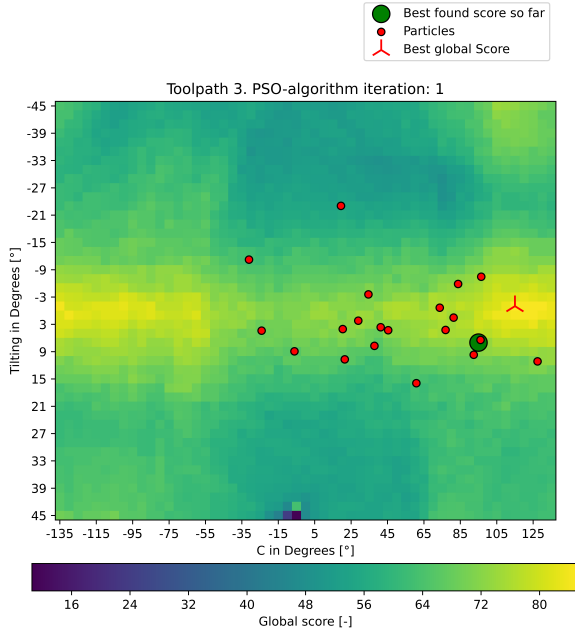


Figure 1.32: PSO Iteration 1 on toolpath 3

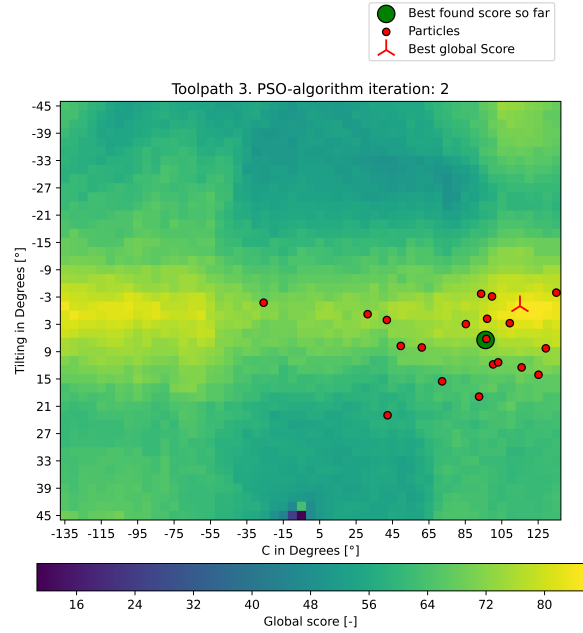


Figure 1.33: PSO Iteration 2 on toolpath 3

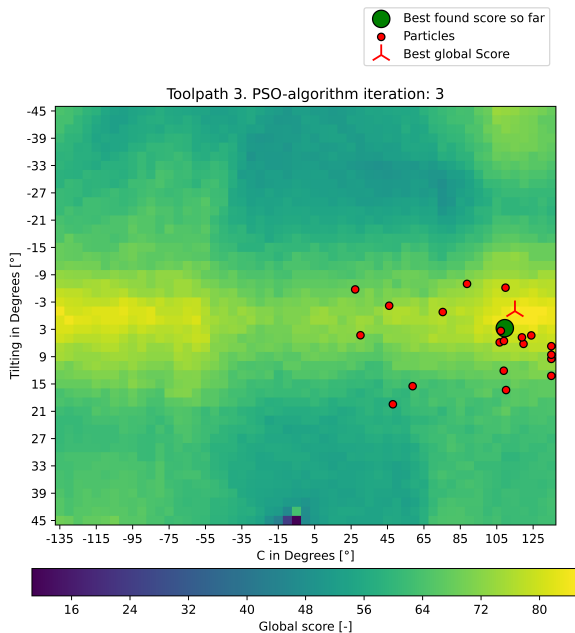


Figure 1.34: PSO Iteration 3 on toolpath 3

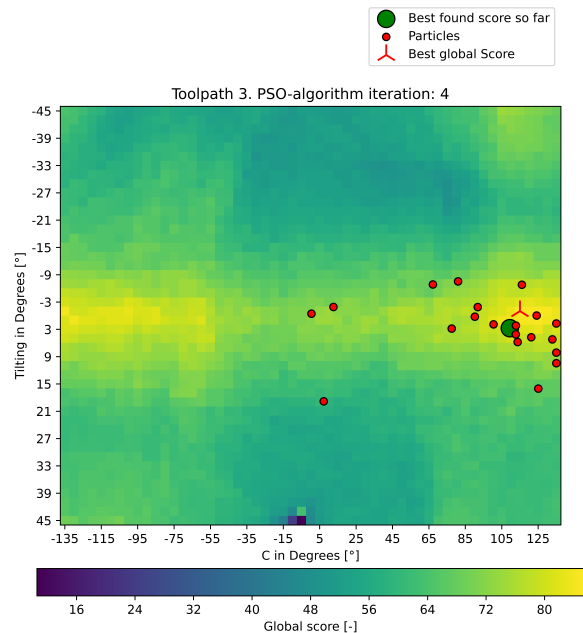


Figure 1.35: PSO Iteration 4 on toolpath 3

The backtracking comparison of all previously visited positions by the particles is clearly evident in the movement of the green dot, which represents the best position found so far. As more points are visited by the particles, the calculation of the best boundary conditions improves. Even without the precalculated global score matrix, the particles are able to converge to the global optimum. Figure 1.36 illustrates the positions of the particles after the fifth and final iteration. It is important to clarify that the global maximum is formed by a plateau and has multiple solutions for the redundant DoF. The red cross marks the first position of

the plateau according to mathematical convention (first row, then column), while the green dot marks the first found maximum. These two positions are not necessarily equal, but they achieve the same global score.

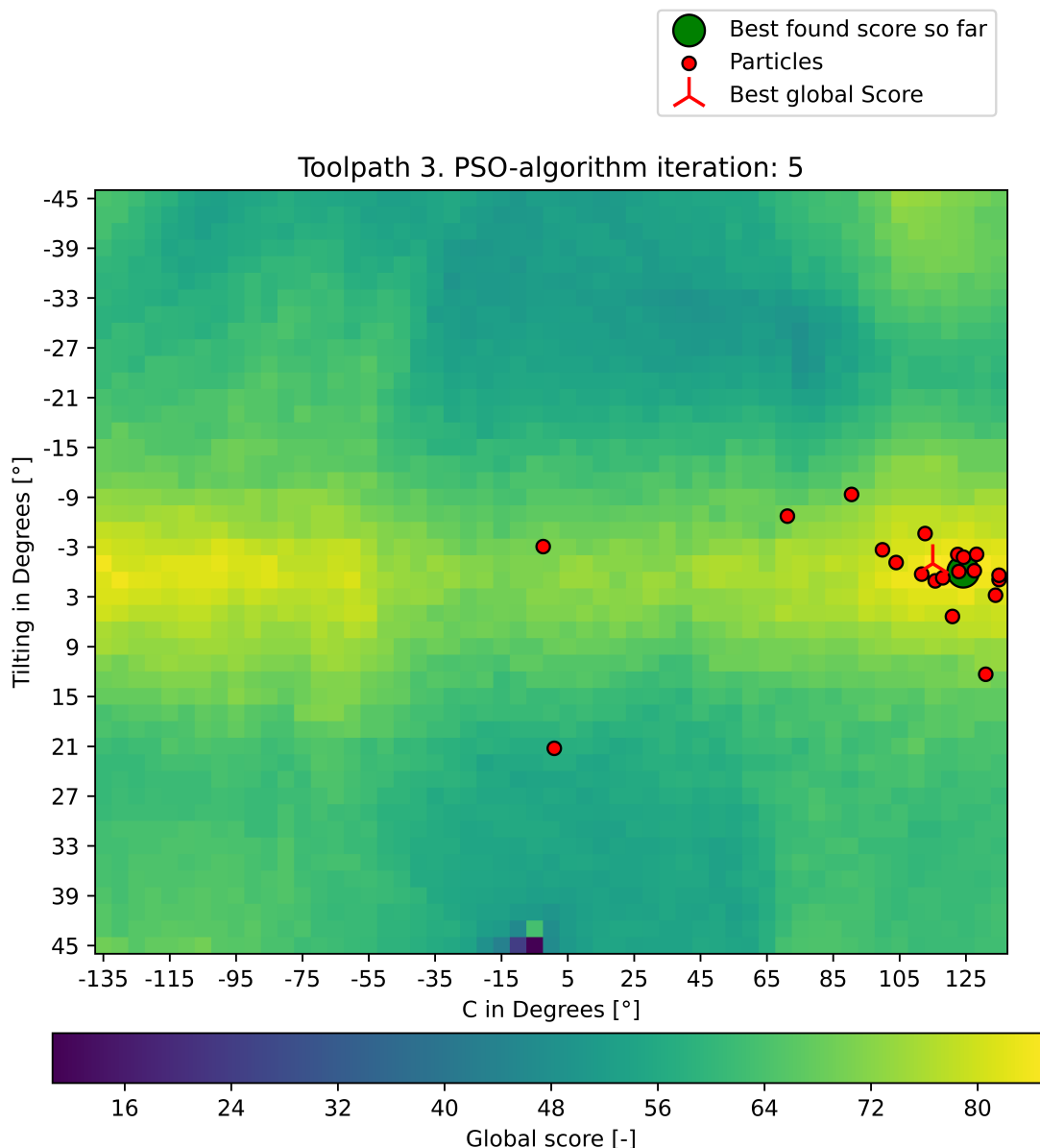
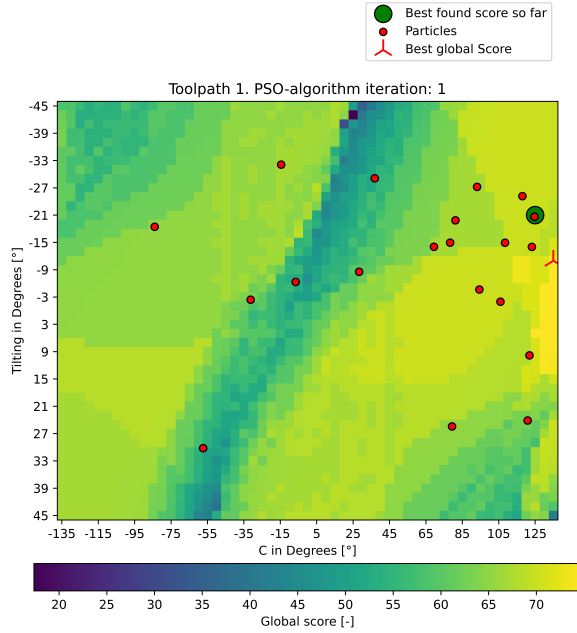
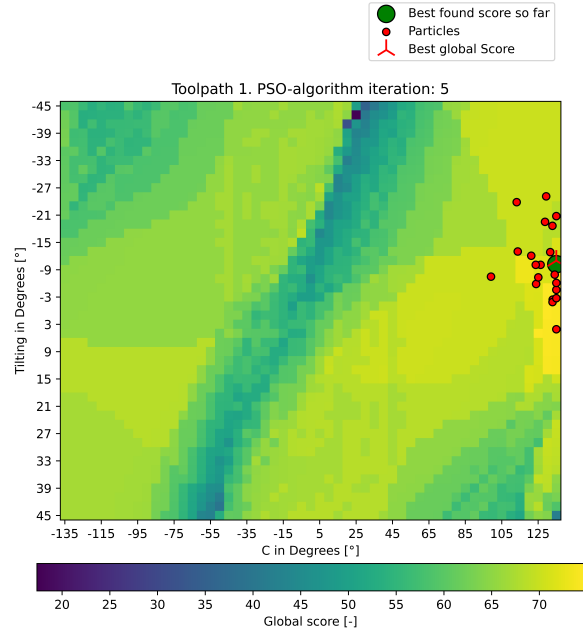
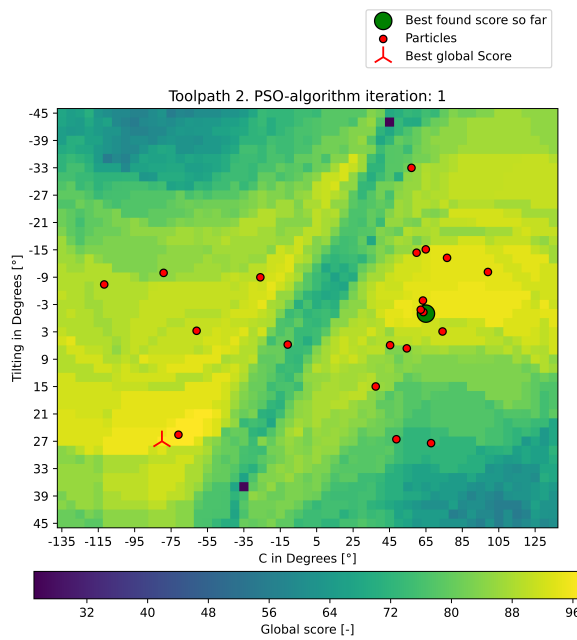
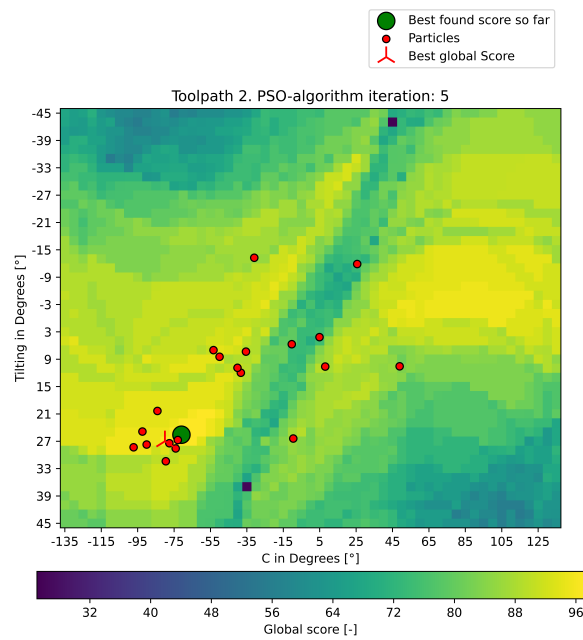


Figure 1.36: PSO iteration 5 on toolpath 3

The same optimization process can be applied to toolpath 1 and toolpath 2. The same process variables and weights are selected as for toolpath 3 (see Table 1.5). Once again, 20 particles are analyzed over 5 iterations. Figures 1.37 and 1.38 depict the positions of the particles after the first and final iteration when analyzing the first toolpath, while Figures 1.39 and 1.40 showcase the initial and final positions of the particles when analyzing the second toolpath. In both cases, the PSO algorithm successfully converges very closely towards the optimal boundary condition.

**Figure 1.37:** PSO Iteration 1 on toolpath 1**Figure 1.38:** PSO Iteration 5 on toolpath 1**Figure 1.39:** PSO Iteration 1 on toolpath 2**Figure 1.40:** PSO Iteration 5 on toolpath 2

1.3 Analysis and Discussion of the Results

In the following, the results of the performed validation are analyzed in detail and critically discussed.

1.3.1 Analysis of the Results

When analyzing only one redundant DoF, specifically the rotation around the Z-axis (see Figure 1.14, Figure 1.15, and Figure 1.16), it becomes evident that there is significant potential for improvement in the robots movement. In this initial test multiple process variables are analyzed. The local score for total travel in all joints and acceleration in joint 1 both exhibit a very continuous change and almost symmetrical behavior over the entire analyzed range. This characteristic is a clear indication that optimization algorithms are a reasonable choice for finding the optimal boundary condition.

To further validate the proposed method for analyzing process variables, a production-grade G-Code is examined (see Figure 1.18). This G-Code consists of 28,000 coordinates and takes significantly longer to analyze. The resulting comparison of all possible values for the redundant DoF shows a fairly smooth curve of the global score. It is important to note that the local score for the direction changes in joint 1 is omitted due to a comparatively small standard deviation. In all other analyzed toolpaths the local score for the direction changes are the least smooth compared to the other analyzed variables.

When considering the scenario where two DoF can be set, it is observed that toolpath 1 and toolpath 2 have a very similar global score matrix (see Figure 1.24 and Figure 1.25). This suggests that these two toolpaths do not differ significantly from each other when considering the process variables alone. A distinct streak is visible in both matrices.

Analyzing the hyperplane of toolpath 3 (Figure 1.23), it is clearly visible that most of the possible combinations result in a global score in the range from 50 to 70. The combinations that lead to a low local score form a single area that is clearly visible in the lower part in the center. Toolpath 3 (Figure 1.23) exhibits an almost symmetrical hyperplane. Two local optima are visible on the left and right sides.

Based on the results obtained from the PSO algorithm (see Figure 1.36), it can be concluded that achieving a close-to-optimal result is feasible when the global score matrix yields smooth surfaces. By implementing this approach, a significant reduction in computation time is possible. Instead of calculating the entire matrix, only 100 toolpaths need to be computed using the inverse kinematics algorithm, resulting in a computation time of just 15 minutes.

The number of particles is selected to be as high as possible while also considering the computational costs. Rather than increasing the number of particles, the number of iterations is set to 5 in order to facilitate convergence towards the global optima. The results clearly show that such a convergence is possible.

In conclusion, the analysis of a single redundant degree of freedom (DoF) revealed significant potential for improvement in the robot's movement. The smooth and symmetrical behavior of process variables suggests that optimization algorithms are suitable for finding the optimal boundary condition. The validation of the proposed method using a production-grade G-Code further supported the effectiveness of analyzing process variables. When considering the scenario with two DoFs, toolpath 1 and toolpath 2 showed similar global score matrices, indicating minimal differences in process variables alone. On the other hand, toolpath 3 exhibited an almost symmetrical hyperplane with visible local optima on both sides. The results obtained from the PSO algorithm demonstrated that achieving close-to-optimal results is feasible when the global score matrix exhibits smooth surfaces. By implementing this approach, a significant reduction in computation time can be achieved. In conclusion, the analysis highlights the potential for improving the robot's movement through optimization algorithms and validates the effectiveness of analyzing process variables. The findings provide valuable insights for optimizing toolpaths and reducing computation time.

1.3.2 Discussion of the Results

Even though the results show a very promising outcome, it is necessary to consider some additional factors. One of the most obvious elements is that only three artificial and one production-grade toolpaths are analyzed. To validate this method in detail, it is necessary to use more real-life production G-code with correctly modeled robotic systems and analyze whether it can be optimized. It should be noted that this work only provides a limited excerpt and does not analyze complex multi-axis operations, which are a significant advantage and building block of the WAAM process.

The selected inverse kinematics algorithm is not designed for optimal high-performance calculations, making it infeasible to use when dealing with toolpaths that have millions of coordinates. Additionally, the algorithm calculates the joint position numerically rather than analytically, which can result in unexpected robot poses. CAM software such as *Siemens NX* or *Master CAM* offer advanced inverse kinematics algorithms that can be used to fine-tune the behavior of the robot.

When analyzing multiple process variables, it is not guaranteed that the resulting surface of the global score matrix will be smooth and optimal for the selected optimization algorithm. Additionally, when working with a PSO algorithm, the final result strongly depends on the initial distribution of the particles. If the optimum is a very tight and sharp spike, the probability of finding the optimal boundary condition is significantly lower. This is particularly true in systems with 3 or more redundant DoF, where simple optimization algorithms can lead to suboptimal results or require unfeasibly long computation times. When implementing the PSO algorithm, 20 particles over 5 iterations are analyzed. In future work, it is necessary to analyze if an increase in population size will improve the convergence rate without significantly impact computation time.

In general, the presented validation does provide a solid basis as a proof of concept for the proposed method. However, additional implementations and tests are necessary for it to be feasible in an industrial environment.

List of Figures

1.1 Schematics of the modeled robot	2
1.2 Visualization of the modeled robot in Python	3
1.3 Toolpath 1: Converging spiral	4
1.4 Toolpath 2: Converging infinity loop	4
1.5 Toolpath 3: Forward moving pendulum oscillation	5
1.6 Traversing toolpath 1 with the modeled robot	5
1.7 Visualization of the joint positions over time for toolpath 1 with C=0°	6
1.8 Visualization of the joint positions over time for toolpath 1 with C=45°	7
1.9 Visualization of the joint positions over time for toolpath 2	7
1.10 Visualization of the joint positions over time for toolpath 3	8
1.11 Toolpath 1 with A=0°, B=0° and C=-45°	9
1.12 Toolpath 1 with A=0°, B=0° and C=45°	9
1.13 Local scores of each process variable for toolpath 1	9
1.14 Global score for toolpath 1	10
1.15 Global and local scores in toolpath 2 depending on the rotation around Z	11
1.16 Global and local scores in toolpath 3 depending on the rotation around Z	11
1.17 Organic toolpath (<i>Reisch 2023</i>)	12
1.18 Global and local score for WAAM toolpath	13
1.19 Global score for production toolpath	14
1.20 Toolpath 3 with no rotation around the X-axis	15
1.21 Toolpath 3 with a rotation of 25 degrees around the X-axis	15
1.22 Robot following the tilted toolpath 3	16
1.23 Hyperplane representing the global score of toolpath 3	17
1.24 Hyperplane representing the global score of toolpath 1	18

1.25 Hyperplane representing the global score of toolpath 2	19
1.26 Distributed of particles at their initial positions	21
1.27 PSO Iteration 2 on toolpath 3	22
1.28 PSO Iteration 3 on toolpath 3	22
1.29 PSO Iteration 4 on toolpath 3	22
1.30 PSO Iteration 5 on toolpath 3	22
1.31 PSO-Loop	23
1.32 PSO Iteration 1 on toolpath 3	24
1.33 PSO Iteration 2 on toolpath 3	24
1.34 PSO Iteration 3 on toolpath 3	24
1.35 PSO Iteration 4 on toolpath 3	24
1.36 PSO iteration 5 on toolpath 3	25
1.37 PSO Iteration 1 on toolpath 1	26
1.38 PSO Iteration 5 on toolpath 1	26
1.39 PSO Iteration 1 on toolpath 2	26
1.40 PSO Iteration 5 on toolpath 2	26

Bibliography

- ABDULHAMEED, O., AL-AHMARI, A., AMEEN, W., and MIAN, S. H., (2019). “Additive manufacturing: Challenges, trends, and applications”. In: *Advances in Mechanical Engineering* 11.2. DOI: 10.1177/1687814018822880.
- AHANGAR, S., MEHRABANI, M. V., POURANSARI SHORIJEH, A., and MASOULEH, M. T., (2019). “Design a 3-DOF Delta Parallel Robot by One Degree Redundancy along the Conveyor Axis, A Novel Automation Approach”. In: *2019 5th Conference on Knowledge Based Engineering and Innovation (KBEI)*. IEEE. DOI: 10.1109/kbei.2019.8734975.
- AMANULLAH, A., MURSHIDUZZAMAN, SALEH, T., and KHAN, R., (2017). “Design and Development of a Hybrid Machine Combining Rapid Prototyping and CNC Milling Operation”. In: 1877-7058 184, pp. 163–170. ISSN: 1877-7058. DOI: 10.1016/j.proeng.2017.04.081.
- ANJUM, Z., SAMO, S., NIGHAT, A., NISA, A. U., SOOMRO, M. A., and ALAYI, R., (2022). “Design and Modeling of 9 Degrees of Freedom Redundant Robotic Manipulator”. In: *Journal of Robotics and Control (JRC)* 3.6, pp. 800–808. ISSN: 2715-5056. DOI: 10.18196/jrc.v3i6.15958. URL: <https://journal.umy.ac.id/index.php/jrc/article/view/15958>.
- ASLAN, D. and ALTINTAS, Y., (2018). “On-line chatter detection in milling using drive motor current commands extracted from CNC”. In: *International Journal of Machine Tools and Manufacture* 132, pp. 64–80. ISSN: 0890-6955. DOI: 10.1016/j.ijmachtools.2018.04.007. URL: <https://www.sciencedirect.com/science/article/pii/s0890695518300841>.
- ATTARAN, M., (2017). “The rise of 3-D printing: The advantages of additive manufacturing over traditional manufacturing”. In: *Business Horizons* 60.5, pp. 677–688. ISSN: 0007-6813. DOI: 10.1016/j.bushor.2017.05.011. URL: <https://www.sciencedirect.com/science/article/pii/s0007681317300897>.
- AYTEN, K. K., SAHINKAYA, M. N., and DUMLU, A., (2016). “Optimum Trajectory Generation for Redundant/Hyper-Redundant Manipulators”. In: *IFAC-PapersOnLine* 49.21, pp. 493–500. ISSN: 2405-8963. DOI: 10.1016/j.ifacol.2016.10.651. URL: <https://www.sciencedirect.com/science/article/pii/s2405896316322637>.
- BÄCK, T. and SCHWEFEL, H.-P., (1993). “An Overview of Evolutionary Algorithms for Parameter Optimization”. In: *Evolutionary Computation* 1.1, pp. 1–23. ISSN: 1063-6560. DOI: 10.1162/evco.1993.1.1.1.
- BANDYOPADHYAY, A., (2020). *Additive Manufacturing, Second Edition*. 2nd ed. Milton: Taylor & Francis Group. ISBN: 9780429881022.

- BEDROSSIAN, N. S., (2002). "Classification of singular configurations for redundant manipulators". In: *Proceedings, IEEE International Conference on Robotics and Automation*. New York: IEEE, pp. 818–823. ISBN: 0-8186-9061-5. DOI: 10.1109/ROBOT.1990.126089.
- BI, Z., (2021). "Computer-Aided Manufacturing (CAM)". In: *Practical Guide to Digital Manufacturing*. Springer, Cham, pp. 223–320. DOI: 10.1007/978-3-030-70304-2{\textunderscore}4. URL: https://link.springer.com/chapter/10.1007/978-3-030-70304-2_4.
- BI, Z. and WANG, X., (2020). *Computer aided design and manufacturing*. 1st edition. Wiley-ASME press series. Hoboken, New Jersey and West Sussex, England: Wiley and ASME Press. ISBN: 9781119534211.
- BIBBY, L. and DEHE, B., (2018). "Defining and assessing industry 4.0 maturity levels – case of the defence sector". In: *Production Planning & Control* 29.12, pp. 1030–1043. DOI: 10.1080/09537287.2018.1503355.
- BILLARD, A. and KRAGIC, D., (2019). "Trends and challenges in robot manipulation". In: *Science* 364.6446. DOI: 10.1126/science.aat8414.
- BONEV, I., (2001). *Delta parallel robot-the story of success*. Newsletter, available at <http://www.parallelmic.org>. URL: <http://www.robotics.caltech.edu/~jwb/courses/me115/handouts/deltarobothistory.pdf>.
- BOSCAROLI, P., CARACCIOLI, R., RICHIEDEI, D., and TREVISANI, A., (2020). "Energy Optimization of Functionally Redundant Robots through Motion Design". In: *Applied Sciences* 10.9, p. 3022. DOI: 10.3390/app10093022.
- BOSCAROLI, P. and RICHIEDEI, D., (2019). "Energy Saving in Redundant Robotic Cells: Optimal Trajectory Planning". In: Springer, Cham, pp. 268–275. DOI: 10.1007/978-3-030-00365-4{\textunderscore}32. URL: https://link.springer.com/chapter/10.1007/978-3-030-00365-4_32.
- BOSE, S., KE, D., SAHASRABUDHE, H., and BANDYOPADHYAY, A., (2018). "Additive manufacturing of biomaterials". In: *Progress in materials science* 93, pp. 45–111. ISSN: 0079-6425. DOI: 10.1016/j.pmatsci.2017.08.003.
- BOSSCHER, P. and HEDMAN, D., (2011). "Real-time collision avoidance algorithm for robotic manipulators". In: *Industrial Robot: An International Journal* 38.2, pp. 186–197. DOI: 10.1108/01439911111106390. URL: <https://www.emerald.com/insight/content/doi/10.1108/01439911111106390/full/pdf>.
- BOUJELBENE, M., MOISAN, A., TOUNSI, N., and BRENIER, B., (2004). "Productivity enhancement in dies and molds manufacturing by the use of C1 continuous tool path". In: *International Journal of Machine Tools and Manufacture* 44.1, pp. 101–107. ISSN: 0890-6955. DOI: 10.1016/j.ijmachtools.2003.08.005.
- BRECHER, C. and LOHSE, W., (2013). "Evaluation of toolpath quality: User-assisted CAM for complex milling processes". In: *CIRP Journal of Manufacturing Science and Technology* 6.4, pp. 233–245. ISSN: 1755-5817. DOI: 10.1016/j.cirpj.2013.07.002. URL: <https://www.sciencedirect.com/science/article/pii/s1755581713000539>.
- BUI, H., PIERSON, H. A., NURRE, S. G., and SULLIVAN, K. M., (2019). "Tool Path Planning Optimization for Multi-Tool Additive Manufacturing". In: 2351-9789 39, pp. 457–464.

- ISSN: 2351-9789. DOI: 10.1016/j.promfg.2020.01.389. URL: <https://www.sciencedirect.com/science/article/pii/s2351978920304601>.
- CALLEJA, A., BO, P., GONZÁLEZ, H., BARTOŇ, M., and LÓPEZ DE LACALLE, LUIS NORBERTO, (2018). "Highly accurate 5-axis flank CNC machining with conical tools". In: *The International Journal of Advanced Manufacturing Technology* 97.5-8, pp. 1605–1615. ISSN: 1433-3015. DOI: 10.1007/s00170-018-2033-7. URL: <https://link.springer.com/article/10.1007/s00170-018-2033-7>.
- Chaurasia *et al.* (2021). Mayank Chaurasia and Manoj Kumar Sinha: Investigations on Process Parameters of Wire Arc Additive Manufacturing (WAAM): A Review. URL: https://www.researchgate.net/publication/348465062_Investigations_on_Process_Parameters_of_Wire_Arc_Additive_Manufacturing_WAAM_A_Review.
- CHEN-GANG, LI-TONG, CHU-MING, XUAN, J.-Q., and XU, S.-H., (2014). "Review on kinematics calibration technology of serial robots". In: *International Journal of Precision Engineering and Manufacturing* 15.8, pp. 1759–1774. ISSN: 2005-4602. DOI: 10.1007/s12541-014-0528-1. URL: <https://link.springer.com/article/10.1007/s12541-014-0528-1>.
- CNC Masters (2022). CNC Machine Buyer's Guide: Types, Uses, Price, & Definitions. URL: <https://www.cncmasters.com/cnc-machine-buyers-guide/>.
- CONG, B., OUYANG, R., QI, B., and DING, J., (2016). "Influence of Cold Metal Transfer Process and Its Heat Input on Weld Bead Geometry and Porosity of Aluminum-Copper Alloy Welds". In: *Rare Metal Materials and Engineering* 45.3, pp. 606–611. ISSN: 1875-5372. DOI: 10.1016/S1875-5372(16)30080-7. URL: <https://www.sciencedirect.com/science/article/pii/s1875537216300807>.
- CUNNINGHAM, C. R., FLYNN, J. M., SHOKRANI, A., DHOKIA, V., and NEWMAN, S. T., (2018). "Invited review article: Strategies and processes for high quality wire arc additive manufacturing". In: *Additive Manufacturing* 22, pp. 672–686. ISSN: 2214-8604. DOI: 10.1016/j.addma.2018.06.020. URL: <https://www.sciencedirect.com/science/article/pii/s2214860418303920>.
- CVITANIC, T., NGUYEN, V., and MELKOTE, S. N., (2020). "Pose optimization in robotic machining using static and dynamic stiffness models". In: *Robotics and Computer-Integrated Manufacturing* 66, p. 101992. ISSN: 0736-5845. DOI: 10.1016/j.rcim.2020.101992. URL: <https://www.sciencedirect.com/science/article/pii/s0736584520302039>.
- DAI, C., LEFEBVRE, S., YU, K.-M., GERAEDTS, J. M. P., and WANG, C. C. L., (2020). "Planning Jerk-Optimized Trajectory With Discrete Time Constraints for Redundant Robots". In: *IEEE Transactions on Automation Science and Engineering* 17.4, pp. 1711–1724. ISSN: 1545-5955. DOI: 10.1109/TASE.2020.2974771.
- Dalton (2024). Imaging CMT Welding with a Weld Camera and Last Access: 05.01.2024. URL: <https://blog.xiris.com/blog/imaging-cmt-welding-with-a-weld-camera>;
- DAS, M. T. and CANAN DÜLGER, L., (2005). "Mathematical modelling, simulation and experimental verification of a scara robot". In: *Simulation Modelling Practice and Theory* 13.3, pp. 257–271. ISSN: 1569-190X. DOI: 10.1016/j.simpat.2004.11.004. URL: <https://www.sciencedirect.com/science/article/pii/s1569190x04001200>.

- DILBEROGLU, U. M., GHAREHPAPAGH, B., YAMAN, U., and DOLEN, M., (2017). “The Role of Additive Manufacturing in the Era of Industry 4.0”. In: *Procedia Manufacturing* 11, pp. 545–554. ISSN: 2351-9789. DOI: 10.1016/j.promfg.2017.07.148. URL: <https://www.sciencedirect.com/science/article/pii/s2351978917303529>.
- DIN EN ISO/ASTM 52900, (2022). In: *Additive Fertigung - Grundlagen - Terminologie (ISO/ASTM 52900:2021); Deutsche Fassung EN ISO/ASTM 52900:2021*. DOI: 10.31030/3290011.
- DING, D., PAN, Z., CUIURI, D., and LI, H., (2015). “Wire-feed additive manufacturing of metal components: technologies, developments and future interests”. In: *The International Journal of Advanced Manufacturing Technology* 81.1-4, pp. 465–481. ISSN: 1433-3015. DOI: 10.1007/s00170-015-7077-3. URL: <https://link.springer.com/article/10.1007/s00170-015-7077-3>.
- DOAN, N. C. N., TAO, P. Y., and LIN, W., (2016). “Optimal redundancy resolution for robotic arc welding using modified particle swarm optimization”. In: *2016 IEEE International Conference on Advanced Intelligent Mechatronics (AIM)*. IEEE. DOI: 10.1109/aim.2016.7576826.
- DOMAE, Y., (2019). “Recent Trends in the Research of Industrial Robots and Future Outlook”. In: *Journal of Robotics and Mechatronics* 31.1, pp. 57–62. ISSN: 1883-8049. DOI: 10.20965/jrm.2019.p0057. URL: https://www.jstage.jst.go.jp/article/jrobomech/31/1/31_57/_article/-char/ja/.
- DUBOVSKA, R., JAMBOR, J., and MAJERIK, J., (2014). “Implementation of CAD/CAM System CATIA V5 in Simulation of CNC Machining Process”. In: *1877-7058* 69, pp. 638–645. ISSN: 1877-7058. DOI: 10.1016/j.proeng.2014.03.037. URL: <https://www.sciencedirect.com/science/article/pii/s1877705814002835>.
- DUONG, X. B., (2021). “On the Effect of the End-effector Point Trajectory on the Joint Jerk of the Redundant Manipulators”. In: *Journal of Applied and Computational Mechanics* 7.3, pp. 1575–1582. ISSN: 2383-4536. DOI: 10.22055/jacm.2021.35350.2635. URL: https://jacm.scu.ac.ir/article_16660.html.
- DUTRA, J. C., GONÇALVES E SILVA, R. H., and MARQUES, C., (2015). “Melting and welding power characteristics of MIG–CMT versus conventional MIG for aluminium 5183”. In: *Welding International* 29.3, pp. 181–186. DOI: 10.1080/09507116.2014.932974.
- Epson (2024). Epson SCARA LS10-B802S/RC-90B | SCARA Robots | Roboter | Produkte | Epson Deutschland and Last Access: 05.01.2024. URL: https://www.epson.de/de_DE/produkte/roboter/scara-robots/epson-scara-ls10-b802s-rc-90b/p/28174.
- ERDŐS, G., KOVÁCS, A., and VÁNCZA, J., (2016). “Optimized joint motion planning for redundant industrial robots”. In: *CIRP Annals* 65.1, pp. 451–454. ISSN: 00078506. DOI: 10.1016/j.cirp.2016.04.024. URL: <https://www.sciencedirect.com/science/article/pii/s0007850616300245>.
- FALUDI, J., BAYLEY, C., BHOGAL, S., and IRIBARNE, M., (2015). “Comparing environmental impacts of additive manufacturing vs traditional machining via life-cycle assessment”. In: *Rapid Prototyping Journal* 21.1, pp. 14–33. DOI: 10.1108/RPJ-07-2013-0067. URL: <https://www.emerald.com/insight/content/doi/10.1108/rpj-07-2013-0067/full/pdf>.

- FARIA, C., FERREIRA, F., ERLHAGEN, W., MONTEIRO, S., and BICHO, E., (2018). “Position-based kinematics for 7-DoF serial manipulators with global configuration control, joint limit and singularity avoidance”. In: *Mechanism and Machine Theory* 121, pp. 317–334. ISSN: 0094-114X. DOI: 10.1016/j.mechmachtheory.2017.10.025. URL: <https://www.sciencedirect.com/science/article/pii/s0094114x17306559>.
- FELDHAUSEN, T., HEINRICH, L., SALEEBY, K., BURL, A., POST, B., MACDONALD, E., SALDANA, C., and LOVE, L., (2022). “Review of Computer-Aided Manufacturing (CAM) strategies for hybrid directed energy deposition”. In: *Additive Manufacturing* 56, p. 102900. ISSN: 2214-8604. DOI: 10.1016/j.addma.2022.102900.
- GADALETÀ, M., PELLICCIARI, M., and BERSELLI, G., (2019). “Optimization of the energy consumption of industrial robots for automatic code generation”. In: *Robotics and Computer-Integrated Manufacturing* 57, pp. 452–464. ISSN: 0736-5845. DOI: 10.1016/j.rcim.2018.12.020. URL: <https://www.sciencedirect.com/science/article/pii/s0736584518301856>.
- GASPARETTO, A. and ZANOTTO, V., (2010). “Optimal trajectory planning for industrial robots”. In: *Advances in Engineering Software* 41.4, pp. 548–556. ISSN: 0965-9978. DOI: 10.1016/j.advengsoft.2009.11.001. URL: <https://www.sciencedirect.com/science/article/pii/s0965997809002464>.
- GHOBAKHLOO, M., (2020). “Industry 4.0, digitization, and opportunities for sustainability”. In: *Journal of Cleaner Production* 252, p. 119869. ISSN: 0959-6526. DOI: 10.1016/j.jclepro.2019.119869. URL: <https://www.sciencedirect.com/science/article/pii/s0959652619347390>.
- GIORGIO BORT, C. M., LEONESIO, M., and BOSETTI, P., (2016). “A model-based adaptive controller for chatter mitigation and productivity enhancement in CNC milling machines”. In: *Robotics and Computer-Integrated Manufacturing* 40, pp. 34–43. ISSN: 0736-5845. DOI: 10.1016/j.rcim.2016.01.006. URL: <https://www.sciencedirect.com/science/article/pii/s0736584516300242>.
- GOEL, R. and GUPTA, P., (2020). “Robotics and Industry 4.0”. In: *A Roadmap to Industry 4.0: Smart Production, Sharp Business and Sustainable Development*. Springer, Cham, pp. 157–169. DOI: 10.1007/978-3-030-14544-6_9. URL: https://link.springer.com/chapter/10.1007/978-3-030-14544-6_9.
- GU, X. and KOREN, Y., (2018). “Manufacturing system architecture for cost-effective mass-individualization”. In: *Manufacturing Letters* 16, pp. 44–48. ISSN: 2213-8463. DOI: 10.1016/j.mfglet.2018.04.002. URL: <https://www.sciencedirect.com/science/article/pii/s2213846317300974>.
- Hagane et al. (2022). Hagane, Shohei and Venture, Gentiane: Robotic Manipulator’s Expressive Movements Control Using Kinematic Redundancy. DOI: 10.3390/machines10121118.
- HÄGELE, M., NILSSON, K., PIRES, J. N., and BISCHOFF, R., (2016). “Industrial Robotics”. In: *Springer Handbook of Robotics*. Springer, Cham, pp. 1385–1422. DOI: 10.1007/978-3-319-32552-1_54. URL: https://link.springer.com/chapter/10.1007/978-3-319-32552-1_54.

- HALEEM, A. and JAVAID, M., (2019). "Additive Manufacturing Applications in Industry 4.0: A Review". In: *Journal of Industrial Integration and Management* 04.04, p. 1930001. ISSN: 2424-8622. DOI: 10.1142/S2424862219300011.
- HALEVI, Y., CARPANZANO, E., MONTALBANO, G., and KOREN, Y., (2011). "Minimum energy control of redundant actuation machine tools". In: *CIRP Annals* 60.1, pp. 433–436. ISSN: 00078506. DOI: 10.1016/j.cirp.2011.03.032.
- HANAFUSA, H., YOSHIKAWA, T., and NAKAMURA, Y., (1981). "Analysis and Control of Articulated Robot Arms with Redundancy". In: *IFAC Proceedings Volumes* 14.2, pp. 1927–1932. ISSN: 1474-6670. DOI: 10.1016/S1474-6670(17)63754-6. URL: <https://www.sciencedirect.com/science/article/pii/s1474667017637546>.
- HEIMANN, O. and GUHL, J., (2020). "Industrial Robot Programming Methods: A Scoping Review". In: *2020 25th IEEE International Conference on Emerging Technologies and Factory Automation (ETFA)*. IEEE. DOI: 10.1109/etfa46521.2020.9211997.
- HESSE, D. F. and MARKERT, B., (2019). "Tool wear monitoring of a retrofitted CNC milling machine using artificial neural networks". In: *Manufacturing Letters* 19, pp. 1–4. ISSN: 2213-8463. DOI: 10.1016/j.mfglet.2018.11.001. URL: <https://www.sciencedirect.com/science/article/pii/s2213846318301524>.
- HEYER, C., (2010). "Human-robot interaction and future industrial robotics applications". In: *2010 IEEE/RSJ International Conference on Intelligent Robots and Systems*. IEEE. DOI: 10.1109/iros.2010.5651294.
- Hoai Nam et al.* (2018). Huynh Hoai Nam, Edouard Riviere, and Olivier Verlinden: Multi-body modelling of a flexible 6-axis robot dedicated to robotic machining. URL: https://www.researchgate.net/profile/huynh-hoai-nam/publication/326106790_multibody_modelling_of_a_flexible_6-axis_robot_dedicated_to_robotic_machining.
- HUO, L. and BARON, L., (2008). "The joint-limits and singularity avoidance in robotic welding". In: *Industrial Robot: An International Journal* 35.5, pp. 456–464. DOI: 10.1108/01439910810893626. URL: <https://www.emerald.com/insight/content/doi/10.1108/01439910810893626/full/pdf>.
- HUYNH, H. N., ASSADI, H., RIVIÈRE-LORPHÈVRE, E., VERLINDEN, O., and AHMADI, K., (2020). "Modelling the dynamics of industrial robots for milling operations". In: *Robotics and Computer-Integrated Manufacturing* 61, p. 101852. ISSN: 0736-5845. DOI: 10.1016/j.rcim.2019.101852. URL: <https://www.sciencedirect.com/science/article/pii/s0736584519301784>.
- IGLESIAS, I., SEBASTIÁN, M. A., and ARES, J. E., (2015). "Overview of the State of Robotic Machining: Current Situation and Future Potential". In: *1877-7058* 132, pp. 911–917. ISSN: 1877-7058. DOI: 10.1016/j.proeng.2015.12.577. URL: <https://www.sciencedirect.com/science/article/pii/s1877705815044896>.
- IQBAL, A., ZHAO, G., SUHAIMI, H., HE, N., HUSSAIN, G., and ZHAO, W., (2020). "Readiness of subtractive and additive manufacturing and their sustainable amalgamation from the perspective of Industry 4.0: a comprehensive review". In: *The International Journal of Advanced Manufacturing Technology* 111.9-10, pp. 2475–2498. ISSN: 1433-3015. DOI: 10.1007/s00170-020-06287-6. URL: <https://link.springer.com/article/10.1007/s00170-020-06287-6>.

- IVÁNTABERNERO, PASKUAL, A., ÁLVAREZ, P., and SUÁREZ, A., (2018). “Study on Arc Welding Processes for High Deposition Rate Additive Manufacturing”. In: 2212-8271 68, pp. 358–362. ISSN: 2212-8271. DOI: 10.1016/j.procir.2017.12.095. URL: <https://www.sciencedirect.com/science/article/pii/s2212827117310363>.
- JAIN, R., NAYAB ZAFAR, M., and MOHANTA, J. C., (2019). “Modeling and Analysis of Articulated Robotic Arm for Material Handling Applications”. In: *IOP Conference Series: Materials Science and Engineering* 691.1, p. 012010. ISSN: 1757-899X. DOI: 10.1088/1757-899X/691/1/012010. URL: <https://iopscience.iop.org/article/10.1088/1757-899x/691/1/012010/meta>.
- JANDYAL, A., CHATURVEDI, I., WAZIR, I., RAINA, A., and UL HAQ, M. I., (2022). “3D printing – A review of processes, materials and applications in industry 4.0”. In: 2666-4127 3, pp. 33–42. ISSN: 2666-4127. DOI: 10.1016/j.susoc.2021.09.004. URL: <https://www.sciencedirect.com/science/article/pii/s2666412721000441>.
- JAYAWARDANE, H., DAVIES, I. J., GAMAGE, J. R., JOHN, M., and BISWAS, W. K., (2023). “Sustainability perspectives – a review of additive and subtractive manufacturing”. In: *Sustainable Manufacturing and Service Economics* 2, p. 100015. ISSN: 2667-3444. DOI: 10.1016/j.smse.2023.100015.
- JI, W. and WANG, L., (2019). “Industrial robotic machining: a review”. In: *The International Journal of Advanced Manufacturing Technology* 103.1-4, pp. 1239–1255. ISSN: 1433-3015. DOI: 10.1007/s00170-019-03403-z. URL: <https://link.springer.com/article/10.1007/s00170-019-03403-z>.
- JIA, Z.-y., MA, J.-w., SONG, D.-n., WANG, F.-j., and LIU, W., (2018). “A review of contouring-error reduction method in multi-axis CNC machining”. In: *International Journal of Machine Tools and Manufacture* 125, pp. 34–54. ISSN: 0890-6955. DOI: 10.1016/j.ijmachtools.2017.10.008.
- JIANG, L., LU, S., GU, Y., and ZHAO, J., (2017). “Time-Jerk Optimal Trajectory Planning for a 7-DOF Redundant Robot Using the Sequential Quadratic Programming Method”. In: 2017, pp. 343–353. DOI: 10.1007/978-3-319-65298-6_32.
- JOSHI, K., MELKOTE, S. N., ANDERSON, M., and CHAUDHARI, R., (2021). “Investigation of cycle time behavior in the robotic grinding process”. In: *CIRP Journal of Manufacturing Science and Technology* 35, pp. 315–322. ISSN: 1755-5817. DOI: 10.1016/j.cirpj.2021.06.021. URL: <https://www.sciencedirect.com/science/article/pii/s1755581721001139>.
- JUNG, J. H. and LIM, D.-G., (2020). “Industrial robots, employment growth, and labor cost: A simultaneous equation analysis”. In: 0040-1625 159, p. 120202. ISSN: 0040-1625. DOI: 10.1016/j.techfore.2020.120202. URL: <https://www.sciencedirect.com/science/article/pii/s0040162520310283>.
- KADAM, O. B., PIRAYESH, A., and FATAHI VALILAI, O., (2023). “Technological Insights of Interoperable Models for Integration of CAD/PLM/PDM and ERP Modules in Engineering Change Management”. In: Springer, Cham, pp. 556–564. DOI: 10.1007/978-3-031-17629-6_58. URL: https://link.springer.com/chapter/10.1007/978-3-031-17629-6_58.

- KAPPMEYER, G. and NOVOMIC, D., (2021). "Production technology research – Building blocks for competitiveness and solution for future challenges in aerospace component manufacturing". In: *2212-8271* 101, pp. 62–68. ISSN: 2212-8271. DOI: 10.1016/j.procir.2020.09.189. URL: <https://www.sciencedirect.com/science/article/pii/s2212827121006570>.
- KATOCH, S., CHAUHAN, S. S., and KUMAR, V., (2021). "A review on genetic algorithm: past, present, and future". In: *Multimedia Tools and Applications* 80.5, pp. 8091–8126. ISSN: 1573-7721. DOI: 10.1007/s11042-020-10139-6. URL: <https://link.springer.com/article/10.1007/s11042-020-10139-6>.
- KIM, H. S. and TSAI, L.-W., (2003). "Design Optimization of a Cartesian Parallel Manipulator". In: *Journal of Mechanical Design* 125.1, pp. 43–51. ISSN: 1050-0472. DOI: 10.1115/1.1543977.
- KIRÉANSKI, M. V. and PETROVIÉ, T. M., (1993). "Combined Analytical- Pseudoinverse Inverse Kinematic Solution for Simple Redundant Manipulators and Singularity Avoidance". In: *The International Journal of Robotics Research* 12.2, pp. 188–196. ISSN: 0278-3649. DOI: 10.1177/027836499301200207.
- KUBELA, T., POCHYLY, A., and SINGULE, V., (2016). "Assessment of industrial robots accuracy in relation to accuracy improvement in machining processes". In: *2016 IEEE International Power Electronics and Motion Control Conference (PEMC)*. IEEE. DOI: 10.1109/epepemc.2016.7752083.
- KUKA (2023). KUKA linear units and Last access: 30.10.2023. URL: <https://www.kuka.com/en-de/products/robot-systems/robot-periphery/linear-units>.
- KUMAR, K., RANJAN, C., and DAVIM, J. P., (2020). *CNC Programming for Machining*. 1st ed. 2020. Materials Forming, Machining and Tribology. Cham: Springer International Publishing and Imprint: Springer. ISBN: 978-3-030-41278-4. DOI: 10.1007/978-3-030-41279-1.
- KUMAR, L. J., PANDEY, P. M., and WIMPENNY, D. I., eds., (2019). *3D Printing and Additive Manufacturing Technologies*. Springer eBook Collection. Singapore: Springer Singapore. ISBN: 9789811303050. DOI: 10.1007/978-981-13-0305-0.
- KYRATSIS, P., KAKOULIS, K., and MARKOPOULOS, A. P., (2020). "Advances in CAD/CAM/CAE Technologies". In: *Machines* 8.1, p. 13. ISSN: 2075-1702. DOI: 10.3390/machines8010013. URL: <https://www.mdpi.com/2075-1702/8/1/13/htm>.
- LALIT NARAYAN, K., MALLIKARJUNA RAO, K., and SARCAR, M. M. M., (2013). *Computer aided design and manufacturing*. Second printing. Delhi: PHI Learning Private Limited. ISBN: 9788120333420.
- LAMBORA, A., GUPTA, K., and CHOPRA, K., (2019). "Genetic Algorithm- A Literature Review". In: *2019 International Conference on Machine Learning, Big Data, Cloud and Parallel Computing (COMITCon)*. IEEE. DOI: 10.1109/comitcon.2019.8862255.
- LI, B., ZHANG, H., and YE, P., (2018). "Error constraint optimization for corner smoothing algorithms in high-speed CNC machine tools". In: *The International Journal of Advanced Manufacturing Technology* 99.1-4, pp. 635–646. ISSN: 1433-3015. DOI: 10.1007/s00170-018-2489-5.

- LI, F., CHEN, S., WU, Z., and YAN, Z., (2018). “Adaptive process control of wire and arc additive manufacturing for fabricating complex-shaped components”. In: *The International Journal of Advanced Manufacturing Technology* 96.1-4, pp. 871–879. ISSN: 1433-3015. DOI: 10.1007/s00170-018-1590-0. URL: <https://link.springer.com/article/10.1007/s00170-018-1590-0>.
- LI, J. Z., ALKAHARI, M. R., ROSLI, N. A. B., HASAN, R., SUDIN, M. N., and RAMLI, F. R., (2019). “Review of Wire Arc Additive Manufacturing for 3D Metal Printing”. In: *International Journal of Automation Technology* 13.3, pp. 346–353. ISSN: 1883-8022. DOI: 10.20965/ijat.2019.p0346. URL: https://www.jstage.jst.go.jp/article/ijat/13/3/13_346/_article/-char/ja/.
- LIBERMAN, Y. L. and GORBUNOVA, L. N., (2021). “Selection of Positioning Devices for the Components of CNC Machines”. In: *Russian Engineering Research* 41.11, pp. 1067–1070. ISSN: 1934-8088. DOI: 10.3103/S1068798X21110204. URL: <https://link.springer.com/article/10.3103/s1068798x21110204>.
- LIN, J., YE, C., YANG, J., ZHAO, H., DING, H., and LUO, M., (2022). “Contour error-based optimization of the end-effector pose of a 6 degree-of-freedom serial robot in milling operation”. In: *Robotics and Computer-Integrated Manufacturing* 73, p. 102257. ISSN: 0736-5845. DOI: 10.1016/j.rcim.2021.102257. URL: <https://www.sciencedirect.com/science/article/pii/s073658452100137x>.
- LIN, Y., ZHAO, H., and DING, H., (2023). “Real-time path correction of industrial robots in machining of large-scale components based on model and data hybrid drive”. In: *Robotics and Computer-Integrated Manufacturing* 79, p. 102447. ISSN: 0736-5845. DOI: 10.1016/j.rcim.2022.102447. URL: <https://www.sciencedirect.com/science/article/pii/s0736584522001302>.
- LIU, C., LI, Y., and HAO, X., (2017). “An adaptive machining approach based on in-process inspection of interim machining states for large-scaled and thin-walled complex parts”. In: *The International Journal of Advanced Manufacturing Technology* 90.9-12, pp. 3119–3128. ISSN: 1433-3015. DOI: 10.1007/s00170-016-9647-4.
- LIU, L., GUO, F., ZOU, Z., and DUFFY, V. G., (2022). “Application, Development and Future Opportunities of Collaborative Robots (Cobots) in Manufacturing: A Literature Review”. In: *International Journal of Human-Computer Interaction*, pp. 1–18. DOI: 10.1080/10447318.2022.2041907.
- LIU, Y., WAN, M., QIN, X.-B., XIAO, Q.-B., and ZHANG, W.-H., (2020). “FIR filter-based continuous interpolation of G01 commands with bounded axial and tangential kinematics in industrial five-axis machine tools”. In: *International Journal of Mechanical Sciences* 169, p. 105325. ISSN: 00207403. DOI: 10.1016/j.ijmecsci.2019.105325.
- Lortek (2023). Fabricación aditiva en metales - WAAM and Last access: 30.10.2023. URL: <https://www.lortek.es/en/technological-areas/metal-additive-manufacturing/waam>.
- MAITI, C. K., (2017). *Introducing technology computer-aided design (TCAD): Fundamentals, simulations and applications*. Temasek Boulevard, Singapore: Pan Stanford Publishing. ISBN: 9789814745529.

- MALYSHEV, D. I., RYBAK, L. A., PISARENKO, A. S., and CHERKASOV, V. V., (2022). "Analysis of the Singularities Influence on the Forward Kinematics Solution and the Geometry of the Workspace of the Gough-Stewart Platform". In: *Advances in Service and Industrial Robotics*. Ed. by MÜLLER, A. and BRANDSTÖTTER, M. Vol. 120. Mechanisms and Machine Science. Cham: Springer International Publishing and Imprint: Springer, pp. 60–67. ISBN: 978-3-031-04869-2. DOI: 10.1007/978-3-031-04870-8{\textunderscore}8.
- Manufacturing Guide* (2023). 5-axis milling, Last access: 30.10.2023. URL: <https://www.manufacturingguide.com/en/5-axis-milling>.
- Mecademic Industrial Robotics* (2023). What are Singularities in a Six-Axis Robot Arm? | Mecademic Robotics and Last access: 02.11.2023. URL: https://www.mecademic.com/academic_articles/singularities-6-axis-robot-arm/.
- MEIER, C., PENNY, R. W., ZOU, Y., GIBBS, J. S., and HART, A. J., (2017). "THERMOPHYSICAL PHENOMENA IN METAL ADDITIVE MANUFACTURING BY SELECTIVE LASER MELTING: FUNDAMENTALS, MODELING, SIMULATION, AND EXPERIMENTATION". In: *Annual Review of Heat Transfer* 20.1, pp. 241–316. ISSN: 1049-0787. DOI: 10.1615/AnnualRevHeatTransfer.2018019042. URL: <https://www.dl.begellhouse.com/references/5756967540dd1b03,562e7b3835dec96e,0860d4f32b9f248d.html>.
- MILENKOVIC, P., (2021). "Wrist singularity avoidance with a robot end-effector adding an oblique, redundant axis". In: *Mechanism and Machine Theory* 162, p. 104355. ISSN: 0094-114X. DOI: 10.1016/j.mechmachtheory.2021.104355. URL: <https://www.sciencedirect.com/science/article/pii/s0094114x21001130>.
- NAGASAI, B. P., MALARVIZHI, S., and BALASUBRAMANIAN, V., (2022). "Effect of welding processes on mechanical and metallurgical characteristics of carbon steel cylindrical components made by wire arc additive manufacturing (WAAM) technique". In: *CIRP Journal of Manufacturing Science and Technology* 36, pp. 100–116. ISSN: 1755-5817. DOI: 10.1016/j.cirpj.2021.11.005. URL: <https://www.sciencedirect.com/science/article/pii/s1755581721001887>.
- NEE, A. Y. C., (2015). *Handbook of Manufacturing Engineering and Technology*. 1st ed. 2015. London: Springer London and Imprint: Springer. ISBN: 978-1-4471-4669-8. DOI: 10.1007/978-1-4471-4670-4.
- NX (2015). Hybrid Additive Manufacturing with NX CAM Overview - NX Manufacturing and Last access: 30.10.2023. URL: <https://blogs.sw.siemens.com/nx-manufacturing/hybrid-additive-manufacturing-with-nx-cam-overview/>.
- OU, W., MUKHERJEE, T., KNAPP, G. L., WEI, Y., and DEBROY, T., (2018). "Fusion zone geometries, cooling rates and solidification parameters during wire arc additive manufacturing". In: *International Journal of Heat and Mass Transfer* 127, pp. 1084–1094. ISSN: 0017-9310. DOI: 10.1016/j.ijheatmasstransfer.2018.08.111. URL: <https://www.sciencedirect.com/science/article/pii/s0017931018323974>.
- PAN, Z., POLDEN, J., LARKIN, N., VAN DUIN, S., and NORRISH, J., (2012). "Recent progress on programming methods for industrial robots". In: *Robotics and Computer-Integrated Manufacturing* 28.2, pp. 87–94. ISSN: 0736-5845. DOI: 10.1016/j.rcim.2011.08.004. URL: <https://www.sciencedirect.com/science/article/pii/s0736584511001001>.

- PARYANTO, BROSSOG, M., BORNSCHLEGL, M., and FRANKE, J., (2015). "Reducing the energy consumption of industrial robots in manufacturing systems". In: *The International Journal of Advanced Manufacturing Technology* 78.5-8, pp. 1315–1328. ISSN: 1433-3015. DOI: 10.1007/s00170-014-6737-z. URL: <https://link.springer.com/article/10.1007/s00170-014-6737-z>.
- PICKIN, C. G., WILLIAMS, S. W., and LUNT, M., (2011). "Characterisation of the cold metal transfer (CMT) process and its application for low dilution cladding". In: *Journal of Materials Processing Technology* 211.3, pp. 496–502. ISSN: 0924-0136. DOI: 10.1016/j.jmatprotec.2010.11.005. URL: <https://www.sciencedirect.com/science/article/pii/s0924013610003456>.
- PICKIN, C. G. and YOUNG, K., (2006). "Evaluation of cold metal transfer (CMT) process for welding aluminium alloy". In: *Science and Technology of Welding and Joining* 11.5, pp. 583–585. DOI: 10.1179/174329306X120886.
- PLOCHER, J. and PANESAR, A., (2019). "Review on design and structural optimisation in additive manufacturing: Towards next-generation lightweight structures". In: *Materials & Design* 183, p. 108164. ISSN: 02641275. DOI: 10.1016/j.matdes.2019.108164.
- PRAKASH, K. S., NANCHARAIH, T., and RAO, V. S., (2018). "Additive Manufacturing Techniques in Manufacturing -An Overview". In: *Materials Today: Proceedings* 5.2, pp. 3873–3882. ISSN: 2214-7853. DOI: 10.1016/j.matpr.2017.11.642. URL: <https://www.sciencedirect.com/science/article/pii/s2214785317329152>.
- R.V. DUBEY, J.A. EULER, and S.M. BABCOCK, (1988). *Robotics and Automation, 5th IEEE International Conference on, 1988: Proceedings*. Los Alamitos: IEEE Computer Society Press. ISBN: 0818608528. URL: <http://ieeexplore.ieee.org/servlet/opac?punumber=202>.
- RAHUL, S. G., DHIVYASRI, G., KAVITHA, P., ARUNGALAI VENDAN, S., KUMAR, K. R., GARG, A., and GAO, L., (2018). "Model reference adaptive controller for enhancing depth of penetration and bead width during Cold Metal Transfer joining process". In: *Robotics and Computer-Integrated Manufacturing* 53, pp. 122–134. ISSN: 0736-5845. DOI: 10.1016/j.rcim.2018.03.013. URL: <https://www.sciencedirect.com/science/article/pii/s0736584517304519>.
- RAMAZANOV, S., BABENKO, V., HONCHARENKO, O., MOISIEIEVA, N., and DYKAN, V., (2020). "Integrated Intelligent Information and Analytical System of Management of a Life Cycle of Products of Transport Companies". In: *Journal of Information Technology Management* 12.3, pp. 26–33. ISSN: 2008-5893. DOI: 10.22059/jitm.2020.76291. URL: https://jitm.ut.ac.ir/article_76291_0.html.
- Reisch (2023). Prozessorientierter Digitaler Zwilling für die Additive Fertigung mittels Lichtbogenauftragschweißen (Dissertation) and Reisch, Raven.
- REITER, A., MULLER, A., and GATTRINGER, H., (2016). "Inverse kinematics in minimum-time trajectory planning for kinematically redundant manipulators". In: *IECON 2016 - 42nd Annual Conference of the IEEE Industrial Electronics Society*. IEEE. DOI: 10.1109/iecon.2016.7793436.
- RUDER, S., (2017). *An overview of gradient descent optimization algorithms*.

- SAXENA, P., STAVROPOULOS, P., KECHAGIAS, J., and SALONITIS, K., (2020). "Sustainability Assessment for Manufacturing Operations". In: *Energies* 13.11, p. 2730. ISSN: 1996-1073. DOI: 10.3390/en13112730. URL: <https://www.mdpi.com/1996-1073/13/11/2730>.
- SCHMITZ, M., WIARTALLA, J., GELFGREN, M., MANN, S., CORVES, B., and HÜSING, M., (2021). "A Robot-Centered Path-Planning Algorithm for Multidirectional Additive Manufacturing for WAAM Processes and Pure Object Manipulation". In: *Applied Sciences* 11.13, p. 5759. DOI: 10.3390/app11135759. URL: <https://www.mdpi.com/2076-3417/11/13/5759>.
- SCOTTI, F. M., TEIXEIRA, F. R., DA SILVA, L. J., ARAÚJO, D. B. de, REIS, R. P., and SCOTTI, A., (2020). "Thermal management in WAAM through the CMT Advanced process and an active cooling technique". In: *Journal of Manufacturing Processes* 57, pp. 23–35. ISSN: 1526-6125. DOI: 10.1016/j.jmapro.2020.06.007. URL: <https://www.sciencedirect.com/science/article/pii/s1526612520303807>.
- SELVI, S., VISHVAKSENAN, A., and RAJASEKAR, E., (2018). "Cold metal transfer (CMT) technology - An overview". In: *2214-9147* 14.1, pp. 28–44. ISSN: 2214-9147. DOI: 10.1016/j.dt.2017.08.002. URL: <https://www.sciencedirect.com/science/article/pii/s2214914717301022>.
- Selvi et al.* (2018). Selvi, S., Vishvaksenan, A., and Rajasekar, E.: Cold metal transfer (CMT) technology - An overview. DOI: 10.1016/j.dt.2017.08.002. URL: <https://www.sciencedirect.com/science/article/pii/s2214914717301022>.
- SHAHZADEH, A., KHOSRAVI, A., ROBINETTE, T., and NAHAVANDI, S., (2018). "Smooth path planning using biclothoid fillets for high speed CNC machines". In: *International Journal of Machine Tools and Manufacture* 132, pp. 36–49. ISSN: 0890-6955. DOI: 10.1016/j.ijmachtools.2018.04.003. URL: <https://www.sciencedirect.com/science/article/pii/s0890695518300804>.
- SHERWANI, F., ASAD, M. M., and IBRAHIM, B., (2020). "Collaborative Robots and Industrial Revolution 4.0 (IR 4.0)". In: *2020 International Conference on Emerging Trends in Smart Technologies (ICETST)*. IEEE. DOI: 10.1109/icetst49965.2020.9080724.
- SHI, X., GUO, Y., CHEN, X., CHEN, Z., and YANG, Z., (2021). "Kinematics and Singularity Analysis of a 7-DOF Redundant Manipulator". In: *Sensors* 21.21, p. 7257. ISSN: 1424-8220. DOI: 10.3390/s21217257. URL: <https://www.mdpi.com/1424-8220/21/21/7257>.
- SICILIANO, B. and KHATIB, O., (2016). *Springer handbook of robotics: With 1375 figures and 109 tables*. 2nd edition. Berlin and Heidelberg: Springer. ISBN: 978-3-319-32550-7. DOI: 10.1007/978-3-319-32552-1.
- Siemens* (2024). Continuous-path mode (G64, G641, G642, G643, G644, G645, ADIS, ADIS-POS) - SINUMERIK ... - ID: 28705635 - Industry Support Siemens and Last Access: 24/10/2023. URL: <https://support.industry.siemens.com/cs/mdm/28705635?c=19192781067&lc=en-AO>.
- SIMONIS, K., GLOY, Y.-S., and GRIES, T., (2016). "INDUSTRIE 4.0 - Automation in weft knitting technology". In: *IOP Conference Series: Materials Science and Engineering* 141.1, p. 012014. ISSN: 1757-899X. DOI: 10.1088/1757-899X/141/1/012014. URL: <https://iopscience.iop.org/article/10.1088/1757-899x/141/1/012014/meta>.

- SINGH, M., FUENMAYOR, E., HINCHY, E., QIAO, Y., MURRAY, N., and DEVINE, D., (2021). “Digital Twin: Origin to Future”. In: *Applied System Innovation* 4.2, p. 36. ISSN: 2571-5577. DOI: 10.3390/asi4020036. URL: <https://www.mdpi.com/2571-5577/4/2/36>.
- SINGH, R., KUKSHAL, V., and YADAV, V. S., (2021). “A Review on Forward and Inverse Kinematics of Classical Serial Manipulators”. In: *Advances in Engineering Design*. Ed. by RAKESH, P. K., SHARMA, A. K., and SINGH, I. Lecture Notes in Mechanical Engineering. Singapore: Springer Singapore and Imprint: Springer, pp. 417–428. ISBN: 978-981-33-4017-6. DOI: 10.1007/978-981-33-4018-3{\textunderscore}39.
- SIVANANDAM, S. N. and DEEPA, S. N., (2007). “Genetic Algorithm Optimization Problems”. In: *Introduction to genetic algorithms*. Ed. by SIVANANDAM, S. N. and DEEPA, S. N. Berlin u.a.: Springer, pp. 165–209. ISBN: 978-3-540-73189-4. DOI: 10.1007/978-3-540-73190-0{\textunderscore}7.
- SRINIVASAN, D., SEVVEL, P., JOHN SOLOMON, I., and TANUSHKUMAAR, P., (2022). “A review on Cold Metal Transfer (CMT) technology of welding”. In: *Materials Today: Proceedings* 64, pp. 108–115. ISSN: 2214-7853. DOI: 10.1016/j.matpr.2022.04.016. URL: <https://www.sciencedirect.com/science/article/pii/s2214785322021289>.
- STEVENSON, R., SHIRINZADEH, B., and ALICI, G., (2002). “Singularity avoidance and aspect maintenance in redundant manipulators”. In: pp. 857–862. DOI: 10.1109/ICARCV.2002.1238536. URL: <https://ieeexplore.ieee.org/abstract/document/1238536>.
- SUN, S. and ALTINTAS, Y., (2021). “A G3 continuous tool path smoothing method for 5-axis CNC machining”. In: *CIRP Journal of Manufacturing Science and Technology* 32, pp. 529–549. ISSN: 1755-5817. DOI: 10.1016/j.cirpj.2020.11.002. URL: <https://www.sciencedirect.com/science/article/pii/s1755581720301280>.
- SVETLIZKY, D., DAS, M., ZHENG, B., VYATSKIKH, A. L., BOSE, S., BANDYOPADHYAY, A., SCHÖENUNG, J. M., LAVERNIA, E. J., and ELIAZ, N., (2021). “Directed energy deposition (DED) additive manufacturing: Physical characteristics, defects, challenges and applications”. In: *Materials Today* 49, pp. 271–295. ISSN: 1369-7021. DOI: 10.1016/j.mattod.2021.03.020. URL: <https://www.sciencedirect.com/science/article/pii/s1369702121001139>.
- TAKEUCHI, Y., (2014). “Current State of the Art of Multi-Axis Control Machine Tools and CAM System”. In: *Journal of Robotics and Mechatronics* 26.5, pp. 529–539. ISSN: 1883-8049. DOI: 10.20965/jrm.2014.p0529. URL: https://www.jstage.jst.go.jp/article/jrobomech/26/5/26_529/_article/-char/ja/.
- TIEN, D. H., DUC, Q. T., VAN, T. N., NGUYEN, N.-T., DO DUC, T., and DUY, T. N., (2021). “Online monitoring and multi-objective optimisation of technological parameters in high-speed milling process”. In: *The International Journal of Advanced Manufacturing Technology* 112.9-10, pp. 2461–2483. ISSN: 1433-3015. DOI: 10.1007/s00170-020-06444-x. URL: <https://link.springer.com/article/10.1007/s00170-020-06444-x>.
- TOMAZ, I., GUPTA, M. K., and PIMENOV, D. Y., (2021). “Subtractive Manufacturing of Different Composites”. In: *Additive and Subtractive Manufacturing of Composites*. Springer, Singapore, pp. 137–165. DOI: 10.1007/978-981-16-3184-9{\textunderscore}6. URL: https://link.springer.com/chapter/10.1007/978-981-16-3184-9_6.

- TUNC, L. T. and STODDART, D., (2017). “Tool path pattern and feed direction selection in robotic milling for increased chatter-free material removal rate”. In: *The International Journal of Advanced Manufacturing Technology* 89.9-12, pp. 2907–2918. ISSN: 1433-3015. DOI: 10.1007/s00170-016-9896-2. URL: <https://link.springer.com/article/10.1007/s00170-016-9896-2>.
- UHLMANN, E., REINKOBER, S., and HOLLERBACH, T., (2016). “Energy Efficient Usage of Industrial Robots for Machining Processes”. In: 2212-8271 48, pp. 206–211. ISSN: 2212-8271. DOI: 10.1016/j.procir.2016.03.241. URL: <https://www.sciencedirect.com/science/article/pii/s2212827116305303>.
- VALENTE, A., BARALDO, S., and CARPANZANO, E., (2017). “Smooth trajectory generation for industrial robots performing high precision assembly processes”. In: *CIRP Annals* 66.1, pp. 17–20. ISSN: 00078506. DOI: 10.1016/j.cirp.2017.04.105. URL: <https://www.sciencedirect.com/science/article/pii/s0007850617301051>.
- VAN LE, T., PARIS, H., and MANDIL, G., (2017). “Environmental impact assessment of an innovative strategy based on an additive and subtractive manufacturing combination”. In: *Journal of Cleaner Production* 164, pp. 508–523. ISSN: 0959-6526. DOI: 10.1016/j.jclepro.2017.06.204. URL: <https://www.sciencedirect.com/science/article/pii/s0959652617313732>.
- VANDE WEGHE, M., FERGUSON, D., and SRINIVASA, S. S., (2007). “Randomized path planning for redundant manipulators without inverse kinematics”. In: *2007 7th IEEE-RAS International Conference on Humanoid Robots*. IEEE. DOI: 10.1109/ichr.2007.4813913.
- WAN, S., LI, X., SU, W., YUAN, J., HONG, J., and JIN, X., (2019). “Active damping of milling chatter vibration via a novel spindle system with an integrated electromagnetic actuator”. In: *Precision Engineering* 57, pp. 203–210. ISSN: 0141-6359. DOI: 10.1016/j.precisioneng.2019.04.007. URL: <https://www.sciencedirect.com/science/article/pii/s0141635918307931>.
- WANG, J., GOYANES, A., GAISFORD, S., and BASIT, A. W., (2016). “Stereolithographic (SLA) 3D printing of oral modified-release dosage forms”. In: *International Journal of Pharmaceutics* 503.1-2, pp. 207–212. ISSN: 0378-5173. DOI: 10.1016/j.ijpharm.2016.03.016. URL: <https://www.sciencedirect.com/science/article/pii/s0378517316302150>.
- WANG, L., LIU, Y., YU, Y., ZHANG, J., and SHU, B., (2022). “Optimization of redundant degree of freedom in robotic milling considering chatter stability”. In: *The International Journal of Advanced Manufacturing Technology* 121.11-12, pp. 8379–8394. ISSN: 1433-3015. DOI: 10.1007/s00170-022-09889-4.
- WANG, W., GUO, Q., YANG, Z., JIANG, Y., and XU, J., (2023). “A state-of-the-art review on robotic milling of complex parts with high efficiency and precision”. In: *Robotics and Computer-Integrated Manufacturing* 79, p. 102436. ISSN: 0736-5845. DOI: 10.1016/j.rcim.2022.102436. URL: <https://www.sciencedirect.com/science/article/pii/s073658452200120x>.
- WATSON, J. K. and TAMINGER, K. M. B., (2015). “A decision-support model for selecting additive manufacturing versus subtractive manufacturing based on energy consumption”. In: *Journal of Cleaner Production* 176, pp. 1316–1322. ISSN: 0959-6526. DOI: 10.1016/j.jclepro.2015.01.010.

- j.jclepro.2015.12.009. URL: <https://www.sciencedirect.com/science/article/pii/s0959652615018247>.
- WEI, Y., JIAN, S., HE, S., and WANG, Z., (2014). “General approach for inverse kinematics of nR robots”. In: *Mechanism and Machine Theory* 75, pp. 97–106. ISSN: 0094-114X. DOI: 10.1016/j.mechmachtheory.2014.01.008.
- Weiss (2024). DR Delta Robots. URL: <https://www.weiss-world.com/gb-en/products/robots-10327/delta-robots-211>; Last Access: %2005.01.2024.
- WICKRAMASINGHE, S., DO, T., and TRAN, P., (2020). “FDM-Based 3D Printing of Polymer and Associated Composite: A Review on Mechanical Properties, Defects and Treatments”. In: *Polymers* 12.7, p. 1529. ISSN: 2073-4360. DOI: 10.3390/polym12071529. URL: <https://www.mdpi.com/2073-4360/12/7/1529>.
- WU, B., PAN, Z., DING, D., CUIURI, D., LI, H., XU, J., and NORRISH, J., (2018). “A review of the wire arc additive manufacturing of metals: properties, defects and quality improvement”. In: *Journal of Manufacturing Processes* 35, pp. 127–139. ISSN: 1526-6125. DOI: 10.1016/j.jmapro.2018.08.001. URL: <https://www.sciencedirect.com/science/article/pii/s1526612518310739>.
- WU, K., LI, J., ZHAO, H., and ZHONG, Y., (2022). “Review of Industrial Robot Stiffness Identification and Modelling”. In: *Applied Sciences* 12.17, p. 8719. DOI: 10.3390/app12178719. URL: <https://www.mdpi.com/2076-3417/12/17/8719>.
- XIONG, G., DING, Y., and ZHU, L., (2019). “Stiffness-based pose optimization of an industrial robot for five-axis milling”. In: *Robotics and Computer-Integrated Manufacturing* 55, pp. 19–28. ISSN: 0736-5845. DOI: 10.1016/j.rcim.2018.07.001. URL: <https://www.sciencedirect.com/science/article/pii/s0736584517304556>.
- XU, T., CHEN, Z., LI, J., and YAN, X., (2015). “Automatic tool path generation from structuralized machining process integrated with CAD/CAPP/CAM system”. In: *The International Journal of Advanced Manufacturing Technology* 80.5-8, pp. 1097–1111. ISSN: 1433-3015. DOI: 10.1007/s00170-015-7067-5. URL: <https://link.springer.com/article/10.1007/s00170-015-7067-5>.
- YANG, B., ZHANG, G., RAN, Y., and YU, H., (2019). “Kinematic modeling and machining precision analysis of multi-axis CNC machine tools based on screw theory”. In: *Mechanism and Machine Theory* 140, pp. 538–552. ISSN: 0094-114X. DOI: 10.1016/j.mechmachtheory.2019.06.021. URL: <https://www.sciencedirect.com/science/article/pii/s0094114x19307992>.
- YANG, J. and YUEN, A., (2017). “An analytical local corner smoothing algorithm for five-axis CNC machining”. In: *International Journal of Machine Tools and Manufacture* 123, pp. 22–35. ISSN: 0890-6955. DOI: 10.1016/j.ijmachtools.2017.07.007.
- YANG, X.-S., (2011). “Metaheuristic Optimization: Algorithm Analysis and Open Problems”. In: Springer, Berlin, Heidelberg, pp. 21–32. DOI: 10.1007/978-3-642-20662-7{\textunderscore}2. URL: https://link.springer.com/chapter/10.1007/978-3-642-20662-7_2.
- YE, W., (2022). “Exploring the Use of Industrial Robots in CNC Machine Tool Programming and Operation Courses”. In: *2022 7th International Conference on Mechatronics System and Robots (ICMSR)*. IEEE. DOI: 10.1109/icmsr2020.2022.00017.

- YUAN, L., PAN, Z., DING, D., HE, F., VAN DUIN, S., LI, H., and LI, W., (2020). “Investigation of humping phenomenon for the multi-directional robotic wire and arc additive manufacturing”. In: *Robotics and Computer-Integrated Manufacturing* 63, p. 101916. ISSN: 0736-5845. doi: 10.1016/j.rcim.2019.101916. URL: <https://www.sciencedirect.com/science/article/pii/s0736584519304260>.
- YUE, C., GAO, H., LIU, X., LIANG, S. Y., and WANG, L., (2019). “A review of chatter vibration research in milling”. In: *1000-9361* 32.2, pp. 215–242. ISSN: 1000-9361. DOI: 10.1016/j.cja.2018.11.007. URL: <https://www.sciencedirect.com/science/article/pii/s1000936119300147>.
- ZHANG, Y., WANG, T., DONG, J., PENG, P., LIU, Y., and KE, R., (2020). “An analytical G3 continuous corner smoothing method with adaptive constraints adjustments for five-axis machine tool”. In: *The International Journal of Advanced Manufacturing Technology* 109.3-4, pp. 1007–1026. ISSN: 1433-3015. doi: 10.1007/s00170-020-05402-x.
- ZHAO, H., ZHANG, B., YIN, X., ZHANG, Z., XIA, Q., and ZHANG, F., (2021). “Singularity Analysis and Singularity Avoidance Trajectory Planning for Industrial Robots”. In: *2021 China Automation Congress (CAC)*. IEEE. doi: 10.1109/cac53003.2021.9727497.
- Zhao et al. (2018). DSCarver: Zhao, Haisen et al. DOI: 10.1145/3197517.3201338.

Disclaimer

I hereby declare that this thesis is entirely the result of my own work except where otherwise indicated. I have only used the resources given in the list of references.

Garching, March 01, 2024

(Signature)